國立交通大學
環境工程研究所

碩士論文

以不同次臨界通量操作之生物薄膜反應槽之薄膜積垢的研究

Membrane fouling under different sub-critical fluxes in membrane bioreactor operation

研究生：阮陳玉富

指導教授：黃志彬、袁如馨 教授

中華民國 100 年 7 月

以不同次臨界通量操作之生物薄膜反應槽之薄膜積垢的研究

Membrane fouling under different sub-critical fluxes in membrane bioreactor operation

研 究 生：阮陳玉富　　Student: Nguyen Tran Ngoc Phu

指導教授：黃志彬　　Advisors: Chihpin Huang

袁如馨　　Jill Ruhsing Pan

國 立 交 通 大 學

環 境 工 程 研 究 所

碩 士 論 文

A Thesis

Submitted to Institute of Environmental Engineering

College of Engineering

National Chiao Tung University

in partial Fulfillment of the Requirements

for the Degree of

Master of Science

in

Environmental Engineering

July 2011

Hsinchu, Taiwan, Republic of China

中華民國 100 年 7 月

以不同次臨界通量操作之生物薄膜反應槽之薄膜積垢的研究

研究生: 阮陳玉富　　指導教授: 黃志彬, 袁如馨 教授

國立交通大學環境工程研究所

摘要

近年來，薄膜過濾系統已被廣泛應用於水回收及廢水處理系統。其中，薄膜生物反應器(membrane bioreactor, MBR)於廢水處理之技術結合了薄膜之物理性過濾及活性汙泥之生物性降解；然而，操作生物薄膜反應器之過程中，薄膜積垢問題常導致操作及物料成本之提高；因此，如何將生物薄膜反應器之薄膜積垢完全去除便成了各國專家學者主要的研究課題。

臨界通量(critical flux)理論發展於 1990 年代中期，其主要之定義為當薄膜生物反應系統中通量控制於臨界通量以下，其清水通量(permeate flux)將不會下降，此值亦稱為次臨界通量(sub-critical flux)。換言之，當操作於次臨界通量之條件下薄膜積垢現象理論上將不會發生；但實際上，薄膜生物反應器中於次臨界通量之條件下操作仍會有積垢之現象產生。

本研究中，臨界通量與逐步通量增加法(flux-step method)之訂定皆須列入考量。其中，親水性膜(HPI membrane)操作於 7,000 – 7,500 mg/l 活性汙泥下之臨界通量為 18 $lm^{-2}h^{-1}$，於 6,000 – 6,500 mg/l 活性汙泥下使用親水膜及疏水性膜(HPO membrane)之臨界通量分別為 33 及 30 $lm^{-2}h^{-1}$。此外，疏水膜於短時間試驗中顯示其較親水膜易形成積垢，薄膜生物反應器中較高之活性汙泥濃度亦較容易造成薄膜積垢現象。於薄膜生物處理系中，胞外聚合物(Extracellular polymeric substance)於薄膜積垢現象中常扮演重要角色，而蛋白質與多醣體為其主要之成分，因此於本研究中蛋白質及多醣體為判別薄膜積垢的重要指標，其薄膜積垢物(foulants)之分析為以 FTIR 進行表面分析，並同時以 EEM 與 CLSM 進行薄膜積垢之特性分析。結果顯示，於垂直分布之分析中，其薄膜表面各物質的濃度皆低於膜上結垢物(cake)表面之濃度，且諸類物質大多分布於積垢物 40-80%之深度位置

關鍵字：薄膜生物反應器、次臨界通量、臨界通量、薄膜積垢、胞外聚合物

Membrane fouling under different sub-critical fluxes in membrane bioreactor operation

Student: Nguyen Tran Ngoc Phu Advisors: Chihpin Huang

Jill Ruhsing Pan

Institute of Environmental Engineering

National Chiao Tung University

Abstract

In recent years, membrane filter has become popular not only in water reuse but also in wastewater treatment. Among them, membrane bioreactor (MBR) is one of the remarkable methods combining membrane filtration and biodegradation of activated sludge for wastewater treatment. Membrane fouling, however, occurred during the operation of MBR process, is considered a major problem causing increased operational cost as well as material cost. Therefore, how to remove membrane fouling has become a big challenge for most researchers interested in MBR in the world.

Critical flux concept has been established in the middle 1990s. The common definition of critical flux is that the permeate flux will not decline if the MBR system is controlled at a flux below critical flux – that is so-called sub-critical flux. In other words, theoretically, fouling will not be observed during sub-critical flux operation. But in practice, membrane fouling still occurs during MBR operation even under sub-critical flux operation.

In this study, to determine critical flux, flux-step method was considered. By which, critical flux for HPI membrane operated with activated sludge of 7,000 – 7,500 mg/l, HPI and HPO membranes under 6,000 – 6,500 mg/l were found at 18, 33 and 30 $lm^{-2}h^{-1}$, respectively. In addition, HPO membrane was fouled much easier than HPI membrane in short-term experiments. A higher propensity of membrane fouling occurred at a reactor with higher sludge concentration. Extracellular polymeric substance plays an important role in causing membrane fouling in MBR. In general, protein and polysaccharide are considered the major compositions of EPS.

Therefore, protein and polysaccharide were identified in this study to indicate membrane fouling. The presence of proteins and polysaccharides in membrane foulants were determined by FTIR analysis. In addition, EEM and CLSM were also used to characterize membrane fouling. Vertical distribution analysis shows that the concentration of fouling substances on the membrane surface is lower than that on cake layer surface. They are distributed from 40% to 80% of the depth of cake layer

Keywords: Membrane bioreactor (MBR), sub-critical flux, critical flux, membrane fouling, Extracellular polymeric substances (EPS).

Acknowledgements

I would like to express my gratitude to my advisors, Prof Chihpin Huang and Prof Jill Ruhsing Pan for the enormous helps given to me. During two years stayed in Taiwan, I have learnt many useful things not only in the studying field but also in the social field. Without the sincere helps, useful advices as well as encouragement from my professors, perhaps I couldn't get these achievements today.

I also want to acknowledge my senior, Dr. Harry Su, who has always accompanied with me during the experimental running. He has helped me how to do the experiment well, how to find a suitable paper for my research at the first time I accustomed to the researching works.

It can be said that granted scholarship from National Chiao Tung University was a great opportunity for me to pursue my studying targets. I wish to thank my university for supporting me in the financial aspect.

Special thanks should go to my seniors – OK, Boting, Wenpin, Zhilin, Jingyi, David, King, Candy, Chacha, James and Phillip for their kindness and friendship during the prolong period of my study in NCTU. Especially, I would like to thank OK again with the great helps of hers from the first days of my life as an international student. Her helps and guidance have helped me to quickly acclimate with the new life in Taiwan.

I am honest to thank my friends - Susu, May, Ivy and Bob for their helps in studying and playing. They have always gone together with me throughout my studying period as well as taught me how to use Chinese efficiently. I am very glad to have sincere friends like you guys.

Many thanks are extended to many of my juniors in Huang group and my friends in other groups in Institute of Environmental Engineering, NCTU for their cooperation during this study.

Finally, I would like to gratitude my parents, my younger sister and my big family for their great compassion and encouragement.

Table of Contents

摘要 i

Abstract ii

Acknowledgements iv

Table of Contents v

List of Tables vii

List of Figures viii

Chapter 1: Introduction 1

1.1 Background 1

1.2 Objectives 2

1.3 Scope of this study 2

Chapter 2: Literature Review 4

2.1 Membrane bioreactors (MBRs) 4

2.1.1 Membrane characteristics 6

2.1.1.1 Membrane materials 6

2.1.1.2 Membrane pore size 7

2.1.2 Membrane fouling 8

2.2 Critical flux and sub-critical flux 11

2.3 Parameters affecting membrane fouling in MBR 13

2.3.1 Effect of membrane hydrophobicity 13

2.3.2 Effect of extracellulose polymeric substance (EPS) 15

2.3.3 Effect of mixed liquor suspended solid (MLSS) 16

Chapter 3: Materials and methods 17

3.1 Materials 17

3.1.1 Membrane bioreactor 17

3.1.2 Feed solution 20

3.2 Methods 21

3.2.1 Flux-step method for determining critical fluxes 21

3.2.2 Preparation of fouling sample 22
3.2.3 MLSS and TOC measurement 23
3.2.4 Examination of Extracellulose Polymeric Substances (EPS) 23
3.2.4.1 Extraction of EPS 23
3.2.4.2 EPS determination 25
3.2.5 Confocal Laser Scanning Spectroscopy (CLSM) 27
3.2.6 Fourier Transform Infrared (FTIR) Spectrophotometer 30
3.2.7 Excitation-Emission Matrix (EEM) method 31
Chapter 4: Results and Discussions 33
4.1 Critical flux determination 33
4.1.1 Flux-step tests 33
4.1.2 Critical and sub-critical flux determination 37
4.1.3 Hysteresis loop for the short-term experiment 41
4.2 TMP change in sub-critical flux operation 43
4.3 Membrane performance under different operation condition 45
4.4 Analysis of membrane fouling 48
4.4.1 Qualitative analysis of foulant 48
4.4.1.1 Detection of EPS compositions by FTIR analysis 48
4.4.1.2 Protein composition of foulant 49
4.4.2 Characterization of fouling composition 56
4.4.3 Distribution of fouling compositions in cake layer 61
Chapter 5: Conclusions and Recommendations 68
5.1 Conclusions 68
5.2 Recommendations 69
References 70
Appendix 1 73
Appendix 2 74
Appendix 3 75

List of Tables

Table 2.1 Characteristics of PVDF flat-sheet membranes used in MBRs 8

Table 2.2 Definition of reversible and irreversible fouling 10

Table 2.3 Contact angle of various membrane materials used in MBRs 14

Table 3.1 Characteristics of applied membrane in this study 19

Table 3.2 Compositions of feed solution as the synthetic wastewater 20

Table 3.3 Summary of dyes with the applied concentration, staining targets, excitation-emission wavelength and indicated color 28

Table 3.4 Wave numbers and functional group of humic substances, polysaccharide and protein in FTIR experiment 30

Table 3.5 Excitation-emission wavelength of the five regions of EEM 32

Table 4.1 Permeability and fouling rate of HPI and HPO membranes in step-flux experiments 40

Table 4.2 Critical flux determination 41

Table 4.3 The average MLSS, TOC in permeate and TOC removal 47

Table 4.4 Peaks location and intensity of membrane fouling compositions 51

Table 4.5 Summary of membrane fouling compositions in different operation conditions 60

List of Figures

Figure 1.1 Scope of this study 3

Figure 2.1 Types of MBRs based on the position of membrane 5

Figure 2.2 Types of MBRs based on the flow directions 5

Figure 2.3 Definition of bound EPS and soluble EPS 15

Figure 3.1 Schematic of the MBR system in this study 17

Figure 3.2 Membrane bioreactors 18

Figure 3.3 Critical flux determinations by flux-step test 21

Figure 3.4 Preparation of fouling sample 23

Figure 3.5 Extraction of EPS from activated sludge in MBRs 24

Figure 3.6 Phenol-Sulfuric acid methods for polysaccharide measurement 25

Figure 3.7 Bradford methods for protein measurement 26

Figure 3.8 Procedure of DNA, protein and polysaccharides staining 29

Figure 3.9 Location of EEM peak based on excitation-emission wavelength 31

Figure 4.1 Critical flux determination of HPI membrane in MBR-1 34

Figure 4.2 Critical flux determination of HPI membrane in MBR-2 35

Figure 4.3 Critical flux determination of HPO membrane in MBR-2 36

Figure 4.4 Comparison of TMP changes between membranes during flux-step trials 36

Figure 4.5 Permeability and fouling rate of HPI membrane in MBR-1 37

Figure 4.6 Permeability and fouling rate of HPI membrane in MBR-2 38

Figure 4.7 Permeability and fouling rate of HPO membrane in MBR-2 39

Figure 4.8 Hysteresis loop for the short-term tests 41

Figure 4.9 Variation of TMP under various sub-critical fluxes operation 43

Figure 4.10 Flat-sheet membranes after long-term sub-critical fluxes operation 44

Figure 4.11 Operational conditions of HPI membrane with 60% of critical flux operated in MBR-1 45

Figure 4.12 Operational conditions of HPO membrane with 80% of critical flux operated in MBR-2 46

Figure 4.13 Operational conditions of HPI membrane with 80% of critical flux operated in MBR-2 46

Figure 4.14 Operational conditions of HPI membrane with 60% of critical flux operated in MBR-2 47

Figure 4.15 FTIR spectra of fouling on membrane surface 48

Figure 4.16 Fluorescent EEM of membrane fouling on HPI membrane operated under 60% critical flux in MBR-1 52

Figure 4.17 Fluorescent EEM of membrane fouling on HPI membrane operated under 80% critical flux in MBR-2 53

Figure 4.18 Fluorescent EEM of membrane fouling on HPO membrane operated under 80% critical flux in MBR-2 54

Figure 4.19 Fluorescent EEM of membrane fouling on HPI membrane operated under 60% critical flux in MBR-2 55

Figure 4.20 Soluble polysaccharides in cake layer and in membrane pore 56

Figure 4.21 Cell-bound polysaccharides in cake layer and in membrane pore 57

Figure 4.22 Soluble proteins in cake layer and in membrane pore 58

Figure 4.23 Cell-bound proteins in cake layer and in membrane pore 59

Figure 4.24 CLSM images of membrane fouling on HPI membrane operated under 60% critical flux in MBR-1 62

Figure 4.25 CLSM images of membrane fouling on HPO membrane operated under 80% critical flux in MBR-2 62

Figure 4.26 CLSM images of membrane fouling on HPI membrane operated under 80% critical flux in MBR-2 63

Figure 4.27 CLSM images of membrane fouling on HPI membrane operated under 60% critical flux in MBR-2 63

Figure 4.28 Vertical distribution of EPS in membrane fouling on HPI membrane operated under 60% critical flux in MBR-1 64

Figure 4.29 Vertical distribution of EPS in membrane fouling on HPO membrane operated under 80% critical flux in MBR-2 65

Figure 4.30 Vertical distribution of EPS in membrane fouling on HPI membrane operated under 80% critical flux in MBR-2 66

Figure 4.31 Vertical distribution of EPS in membrane fouling on HPI membrane operated under 60% critical flux in MBR-2 67

Chapter 1

Introduction

1.1 Background

The exponential increase in world population together with the industrialization all over the world results in a skyrocketing increase in daily water use and the resultant wastewater into the environment. It gradually deteriorates the quality of surface and groundwater if without proper treatment scheme.

Membrane bioreactors system has been considered as a potential effective method for treating wastewater because of many advantages over the conventional activated sludge treatment processes. MBRs provide a high treated water quality, reaching to the strict standards in all countries. Beside that, flexibility in operation, small footprint, low rate sludge production, high rate decomposition or effective in disinfection and odor control have also been recognized. However, membrane fouling has become a major cause, impeding its widespread applications.

The purpose of setting up a waste water treatment system is to treat wastewater discharged from different sources such as industrial wastewater and municipal wastewater. However, to get a success in wastewater treatment systems, the engineers are required to understand deeply about not only the system structure but also the operational mechanisms of each certain step in the treatment process. Therefore, to understand more about membrane fouling is required for operating the MBRs system effectively, especially in a field of membrane fouling under sub-critical flux operation.

Critical flux was introduced as a limit point at which membrane fouling rate is zero. According to this concept, it was said that membrane fouling during MBRs process will not occur at theoretical point of view under sub-critical flux operation. But in practice, membrane fouling always occurs under whether sub-critical flux operation or super-critical flux operation. Operated under step-flux method was applied for finding out the critical flux and then the MBR was sub-critical flux condition. Two types of membranes, hydrophilic and hydrophobic PTFE, were used.

In this investigation, the systems were performed under different MLSS concentration. Critical flux was firstly found and sub-critical fluxes also were calculated with 60% and 80% of critical flux. Then, the MBR system was operated with the given sub-critical flux to identify the critical factors for fouling during sub-critical flux operation. EPS compositions were determined for elucidating the main cause of membrane fouling during this stage.

1.2 Objectives

The main purposes of this research were:

- To find out the critical flux of each type membrane
- To investigate the occurrence of membrane fouling under different sub-critical fluxes operation, to analyze the composition of fouled membrane, and to investigate the causes for membrane fouling
- To compare between the MBR performances of the membrane under sub-critical flux operation.

1.3 Scope of this study

Figure 1.1 shows the scope of this study in which the membrane fouling under different sub-critical flux operation were considered. First step of this study was to identify the critical flux of HPI and HPO membrane operated under different operational conditions. After found out the critical flux, sub-critical fluxes were calculated with 60% and 80% of critical flux. In case of operating the MBR system by 60% of critical flux, HPI membranes were chosen for performing in different activated sludge (AS) concentrations (7,000 – 7,500 mg-MLSS/l and 6,000 – 6,500 mg-MLSS/l). The MBR operated with AS of 7,000 – 7,500 mg-MLSS/l was abbreviated as MBR-1. Another was MBR-2. In case of operating the MBR system by 80% of critical flux, MBR-2 was chosen to carry out the test with HPI and HPO membrane. After finishing the long-term test, EPS concentration, particle size distribution, FTIR, CLSM and EEM methods were applied to determine the fouling behavior in each case.

A comparison between HPI and HPO membrane operated under 80% critical flux in MBR-2; HPI membranes operated in MBR-2 with different sub-critical flux (60% and

80% of critical flux) and HPI membrane operated under the same sub-critical flux in MBR-1 and MBR-2 were also performed to identify the critical factors for fouling during sub-critical

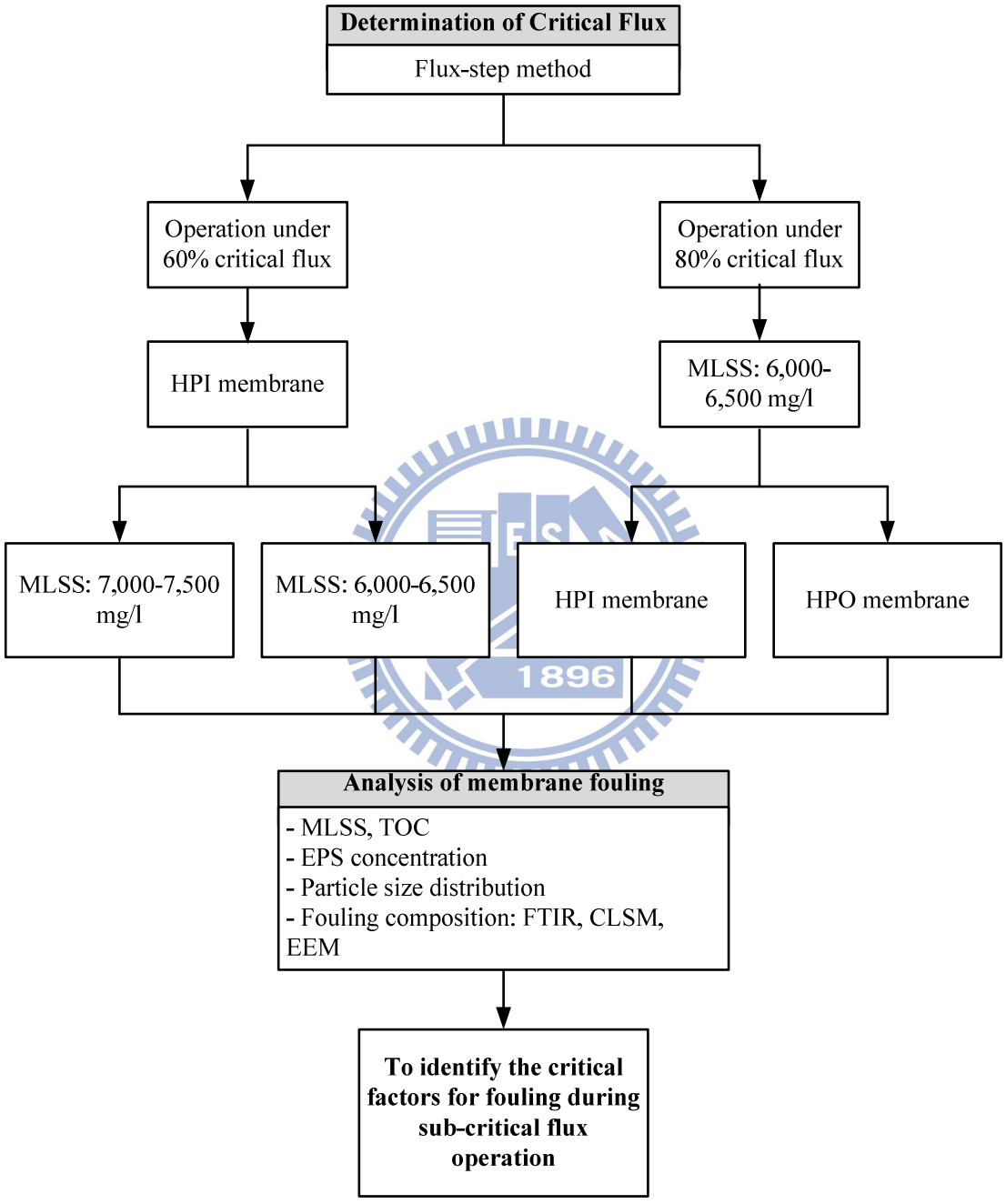

Figure 1.1 Scope of this study

Chapter 2

Literature Review

When the conventional wastewater treatment system no longer meets the stringent standards in an effort to preserve natural water resources, the emerging technology for wastewater treatment has become an urgent requirement for supplying the clean water for daily demands or discharging into the receiving sources such as lake, river, ground water or any other receiving sources. Membrane bioreactors (MBRs) offering several advantages over the conventional processes have gradually been used for satisfying these requirements in each country all over the world. Unfortunately, membrane fouling causing the decline of membrane performance leading to the increasing of operational cost has been preventing the widespread of this application. In this chapter, some concepts relating to MBRs as well as membrane fouling will be introduced.

2.1 Membrane bioreactors (MBRs)

By the late 1960s, a commercialized MBRs process was firstly introduced by Dorr-Oliver with the use of an activated sludge bioreactor coupled a cross-flow membrane (Smith *et al.*, 1969). Due to a poor industrial development in producing a good performance of membrane at that time, the cost of membrane, obviously, was very high. Beside that, to reduce fouling occurring in MBRs process, the mixed liquor suspension in the activated sludge bioreactor was pumped at high velocity at considerable energy (up to 10 kWh per 1 m^3 of water product) (Le-Clech *et al*., 2006). As a result, the first generation of MBRs couldn't be applied as an emerging technology. Up to 1989s, the Japanese Government co-operated with many large companies to find out a new direction for implementing a better process for water recycling. Kubota company - a participate member of above cooperation- proposed and developed a flat-sheet submerged MBR. Yamamoto and his co-worker have pioneered in running a submerged MBR with hollow fiber membrane in this time (Yamamoto *et al*., 1989). The new era of using MBRs in treating wastewater has been opened ever since then

In general, MBRs are a technology combined between a direct filtration of a selectively permeable membrane and the biological degradation of activated sludge in a

wastewater treatment system. The solvent liquid is separated from the solution through membrane by a certain driving force based on the using purpose of the operational workers. According to the operational mode, MBRs were basically divided into two subgroups: bioreactors with membrane in external circuit and bioreactor with submerged membrane (Visvanathan *et al.,* 2000). Bioreactors with membrane in external circuit appeared in the beginning of using membrane in wastewater treatment. Because of its inconvenience in operation as well as in operational cost, nowadays, no more authors have mentioned to this approach in their researches. In contrary, most MBRs design for wastewater treatment has been focused on the submerged membrane bioreactors. The fouling will easily be removed by shear stress caused air bubbles from aeration. Nevertheless, the operating cost as well as fouling-cleaning cost will decrease compared to the external circuit membrane bioreactor. A general setup of two types of membrane bioreactors is presented in Figure 2.1.

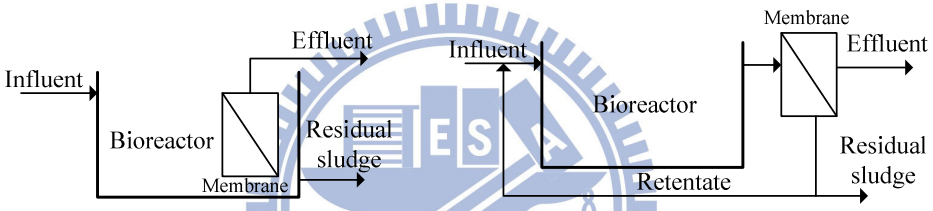

(a) Submerged MBR (b) External circuit MBR

Figure 2.1 Types of MBRs based on the position of membrane

In addition, with different direction of feed flow, concentrate or permeate, MBRs can also be categorized into dead-end filtration and cross-flow filtration. In case of dead-end filtration, the feed flow perpendicularly moves to the membrane surface. By this way, the fouling easily deposits onto the membrane surface. Then, the operator will often replace the membrane modules. Regarding to cross-flow filtration, the feed flow moves parallel with the surface of membrane. This way is considered as a natural method to mitigate the membrane fouling without stopping the system. Figure 2.2 illustrates the two concepts above.

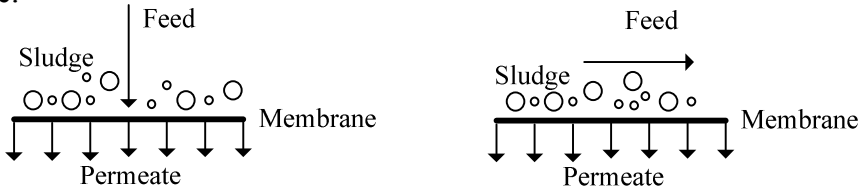

(a) Dead-end filtration (b) Cross-flow filtration

Figure 2.2 Types of MBRs based on the flow directions

2.1.1 Membrane characteristics

Membrane characteristics are considered as the factors that contribute to the success of MBR performance such as the pore size of membrane, hydrophobic or hydrophilic membrane or membrane morphology. These mentioned factors affect membrane fouling propensity (Madaeni *et al.*, 1999; Le-Clech *et al*., 2003b; Maximous *et al.*, 2009) and resultantly affect the performance of MBR system. The extent of this part is to introduce some basic information about membrane material, membrane pore size and hydrophobic/hydrophilic characteristic of membrane.

2.1.1.1 Membrane materials

A membrane classification is conveniently accordant to the composition which formed the membranes. To perform with an optimal efficiency, many types of membranes have been experimented either in real MBR systems or in experimental MBR systems. During 50 years of development and application, two different types of materials, organic/polymeric materials and inorganic/ceramic materials, are used to form membranes served in many purposes of water fields *(*Judd, 2006*)*. Polymeric membranes are noted as the preferred membranes in membrane system. Ceramic membranes have been successfully applied for several kind of wastewater, such as treatment of high-strength industrial waste and anaerobic applications (Le-Clech *et al.,* 2006). However, as mentioned above, ceramic membrane cannot be used as a popular option due to the high cost compared to polymeric membranes. In conclusion, a suitable membrane materials should have some special feature to stand with the conditions of MBR system such as having a strong resistance to thermal and chemical attack, high temperature, high or low pH in the reactors and low cost. Stephenson *et al*. (2000) has released some membrane materials by name and simultaneously presents the advantages and disadvantages of it.

With the development of technology, the cost of membrane is day-by-day decreasing. This becomes one of the most advantages of MBR system to invest many MBR plants in most of countries even in the developing countries.

2.1.1.2 Membrane pore size

A range of membrane pore size used in lab-scale experiments mainly lies from 0.02 to 0.5 µm (Stephenson *et al.,* 2000). In a submerged flat sheet system, Stephenson also showed the dependence of the decline rate of flux against membrane pore size. Membrane pore size strongly effects to the performance of membrane by rejecting the higher size of colloid, suspended solid etc…in the sludge solution that tend to form a cake layer on the membrane surface caused the decline of the effluent flux. Gander *et al*. (2000) revealed that the initial fouling of the larger membrane pore size dominated over the smaller pore size when conducting a series of membranes with different pore size from 0.4 to 5 µm.

It was reported that the blocking index of 0.4 µm of membrane pore size was always higher than that of 0.2 µm under the same operational conditions (Hwang *et al.,* 2008). Beside that, many researchers have focused on the optimal performance of membrane pore size. Choo and Lee (1996) proposed that membrane with 0.1 µm pore size have a best performance with the least membrane fouling tendency compared to other 0.02, 0.5 and 1 µm of membrane pore size. A study related to the influence of four membrane types (cellulose acetate, polyethersulfone, mixed ester, polycarbonate) with three different pore sizes (0.40 – 0.45, 0.22, 0.10 µm) on cross-flow filtration was conducted by Nadir Dizge and his colleagues. In this study, cellulose acetate membrane with pore size of 0.45 µm presented a worst performance with the most rapid decline of flux among all membranes.

Some authors have found that membrane pore size exhibits a negative effect to the critical flux with the pore size from 0.01 to 0.1µm (Le-Clech *et al.,* 2003a). Madaeni (1999) supposed that the critical flux of membrane was not dependent on the membrane pore size (although the TMP is different with the difference of the pore size). In other words, according to Madaeni, the larger the pore size, the higher the TMP produced although the flux is the same with all cases.

Table 2.1 shows the characteristics of PVDF flat-sheet membranes used in MBRs by many authors in order to making a relationship between critical flux and membrane characteristics.

Table 2.1 Characteristics of PVDF flat-sheet membranes used in MBRs

Pore size (μm)	J_c ($Lm^{-2}h^{-1}$)	MLSS (g/L)	Hydrophobicity	References
0.45	67	4	HPI	Madaeni *et al*. (1999)
0.22	62	4	HPO	Madaeni *et al*. (1999)
0.22	50	0.3-0.5	HPI	B.D.Cho *et al*. (2002)
0.2	32-38	-	-	Wang *et al*. (2008)
0.2	38	3.2-5.5	HPI	Wu *et al.* (2008)

2.1.2 Membrane fouling

The development of membrane fouling in a membrane bioreactor is one of the main causes for flux decline during long-term operation, preventing the wide-spread application of MBR in the wastewater treatment. It is caused by the deposition or attachment of small particles such as colloids, solutes, microorganisms, cells-debris and biomass residuals on the membrane surface. Membrane fouling mitigation has been investigated to improve the performance of membrane, and to decrease the operational cost. The carbohydrate fraction from the soluble microbial product has been accepted as the major fouling in membrane bioreactors (Clech *et al.,* 2006; Pan *et al,* 2008). In which, hydrophilic carbohydrates are the predominant cause for membrane fouling (Pan *et al*., 2008). Another study has mentioned that the fatty acids from bacterial lipopolysaccharides are mainly related to membrane fouling (Al-Halbouni *et al*., 2008). Zhang *et al* (2006) observed the membrane fouling that follows a three stage fouling history. Stage 1 is an initial short-term rise in transmembrane pressure. Stage 2 is a long-term TMP rise or a slow fouling stage. Stage 3 is that the transmembrane pressure suddenly jump due to the fouling exceedingly deposited on the membrane surface. A review of Meng *et al*. (2008) has summarized the membrane fouling mechanisms as following:

- Adsorption of solutes or colloids
- Deposition of sludge flocs
- Formation of a cake layer
- Detachment of fouling caused by shear forces
- The spatial and temporal changes of the fouling composition

Particle size plays a significant role in categorizing membrane. Three type of membrane fouling are proposed: adsorption, pore blocking and cake layer (Hong *et al.,* 2005). With the complex compositions of membrane fouling such as colloids, solutes .etc, size of some sludge particles that is smaller than the membrane pore size tends to adsorb on pore wall and gradually fulfill the membrane pore. In a case of the sludge particle size is as same as membrane pore size, the foulants will block the membrane pore. It is called as pore blocking. Both adsorption and pore blocking are considered as irreversible fouling (Chang *et al., 2002;* Drews 2010) or irremovable fouling (Meng *et al*., 2009).

Cake layer is formed on membrane surface only when the size of sludge particle is much larger than that of membrane. A cake layer is a complex system of the interaction between not only colloids-colloids, solutes-solutes, solutes-colloids but also colloids, solutes-membrane surface. The cake layer which contributes 80% of total resistance of membrane system mainly affects to the membrane fouling formation (Lee *et al.,* 2001). Fortunately, many researches have pointed out that cake layer is removable from the membrane surface by physical cleaning as well as is removed by shear-stress caused by aeration supported during the running of membrane bioreactors (Chu *et al.,* 2004; Chang *et al.,* 2002; Le-Clech *et al.,* 2006; Meng *et al.,* 2009; Drews 2010).

According to the removable characteristics of membrane fouling on the membrane surface, many scientists have mentioned to membrane fouling as reversible and irreversible fouling. Reversible fouling is a type of membrane fouling that is easy to be removed by physical washing such as back flushing or relaxation. On the other hand, irreversible fouling is generally removed by chemical cleaning (Chang *et al.,* 2002). However, Meng *et al*. (2008) supposed that there is existing some types of membrane fouling that neither physical washing nor chemical cleaning can be used to remove. Therefore, these authors defined three types of fouling that are removable fouling, irremovable fouling and irreversible fouling. The term of irrecoverable fouling has been proposed by Drews (2010) in which this type of membrane fouling can't be removed by any cleaning means. This definition is familiar with the definition of Meng *et al*. (2008) about irreversible fouling. Table 2.2 shows various definition of reversible and irreversible fouling occurred during MBR operation.

Table 2.2 Definition of reversible and irreversible fouling

Cleaning methods	The term of fouling	References
Physical cleaning	Reversible fouling	Drews, (2010)
		Chang *et al*. (2002)
	Removable fouling	Meng *et al*. (2009)
Chemical cleaning	Irreversible fouling	Drews, 2010
		Chang *et al.* (2002)
	Irremovable fouling	Meng *et al.* (2009)
None(*)	Irrecoverable fouling	Drews, (2010)
	Irreversible fouling	Meng *et al.*(2009)

(*) no suitable methods used to remove fouling

Regarding to the constituents of membrane fouling, fouling can be classified into biofouling, organic fouling and inorganic fouling (Meng *et al.,* 2009). For a long-term operation, a microbial biofilm occurs on the membrane surface due to an interaction between microbial community and membrane surface. This microbial biofilm is the accumulation of cells and microorganisms products. In other words, the free-floating microorganisms lived in the sludge solution will colonize the membrane surface by attaching on the surface and develop their biomass. The so-called "biofouling" is also referred to this microbial biofilm and all products excreted from the microbial community activities that effect to the performance of membrane systems. Biofouling is still inevitable due to the complex characteristics of microbial system (Le-Clech *et al.,* 2006).

The term of organic fouling refers to the adsorption of organic matters on the membrane surface and its pore inside due to the small size of particle and suction force pump in the system. Biopolymers such as proteins and polysaccharides are predominant in organic fouling compositions and dependent on the Food/Microorganism (F/M) ratio in which high F/M make the fouling more proteinaceous (Kimura *et al*., 2005).

Inorganic fouling contributes a small role in membrane resistance due to the low concentration in the activated sludge solution. The inorganic fouling is formed from the chemical precipitation and biological precipitation. Metal ions can easily react with the specific functional group of biopolymer such as CO_3^{2-}, SO_4^{2-} (Meng *et al.*, 2009)… and deposited on the cake layer. Otherwise, inorganic fouling is also able to adsorb into the membrane pore and become the irreversible fouling. Chemical cleaning is predominant in removal of the inorganic precipitate compared to the physical cleaning.

2.2 Critical flux and sub-critical flux

The term "flux" refers to how much of clean water that flows through a unit area of membrane per unit time. When running the membrane system, the flux is determined by the following equation seen as an integral form of Darcy law (Bacchin *et al.,* 2006).

$$J = \frac{\Delta P - \Delta \pi}{\mu(R_m + R_{ads} + R_{rev} + R_{irrev})} \qquad (2.1)$$

Where:

J: Permeate flux ($m^3m^{-2}h^{-1}$)

ΔP: A transmembrane pressure (Pa)

$\Delta \pi$: An osmotic pressure (Pa)

μ: Viscosity (Pa.s)

R_m is the resistance of original membrane; R_{ads} is the resistance caused by surface or pore adsorption; Irreversible fouling R_{irrev} is caused by cake deposit or gel formation; Reversible fouling R_{rev} is caused by pore linking or cake deposit.

Critical flux plays an important role in operating a certain membrane bioreactor. The engineer should controls the system based on critical flux for an effective operation. Critical flux plays an important role in characterizing the membrane fouling as well as the membrane bioreactor performance. One definition for critical flux is that *"The critical flux for MF is that on start-up there exists a flux below which a decline of flux with time does not occur; above it fouling is observed. This flux is the critical flux and its value depends on the hydrodynamics and probably other variables"* (Field *et al.,* 1995). The other definition is that the flux below which colloids do not deposit on the membrane surface (Howell, 1995). By these two definitions, membrane fouling will be noticeable at

a flux called “critical flux”. Above the critical flux, all type of activated sludge compositions such as colloids, suspended solid … will quickly attach on the membrane surface caused the rapid decline in flux. The term sub-critical refers to the flux below which the fouling does not. Otherwise, the strong form and weak form of critical fluxes have been developed to compare with the conventional definition (Bacchin *et al.,* 2006). The strong form of critical flux is defined as the flux point at which the transmembrane pressure curve changes direction from linearity with the assumption of the absence of adsorption and osmotic pressure. In the presence of adsorption, the definition of the weak form of critical flux is also the same with that of the strong form of critical flux but the steady-state is different from that of pure water. Up to now, a standardized methodology has not yet been designed for exactly determining the value of the weak form of critical flux (Guglielmi *et al.,* 2006)

Numerous methods for identifying the critical flux of a certain membrane have been proposed by a number of authors that whose research focused on the membrane area (Le-Clech *et al.,* 2003a; Espinasse *et al.,* 2002). Pierre Le-Clech and his colleagues have established the concept of flux-step method in 2003 (Le-Clech *et al.,* 2003a). Flux-step method is a common method developed for determining the critical flux of membrane used in a membrane bioreactor operating at constant flux. During the flux-step test, smaller step height is required to make the test precisely (Tiranuntakul *et al.,* 2011). Some specific hydraulic parameters obtained from this experiment such as the initial transmembrane pressure increase (ΔP_0), the rate of transmembrane pressure increase (dP/dt), permeability (K), and the average transmembrane pressure (P_{ave}) are used to identify critical flux (Le-Clech *et al.,* 2003b). This author also defined critical flux the flux at which permeability decreases to below 90% of initial permeability recorded for the first filtration step. In another paper, Guglielmi *et al.* (2006) proposed critical flux is the flux at which the initial permeability is higher than 90% of the initial permeability. The concentration of feed-solution, shear rate and membrane characteristics affect the value of critical flux. The critical flux has been found higher at higher cross-flow velocity, lower feed concentration and lower for hydrophobic membrane (Madaeni *et al.,* 1999).

2.3 Parameters affecting membrane fouling in MBR

2.3.1 Effect of membrane hydrophobicity

An interaction between feed solution and membrane existing with two major classes: An interaction between the water and membrane and an interaction between the solutes in the water and membrane. The so-called "hydrophilicity" is referred to the high affinity of membrane surface against the water, while the low affinity is called "hydrophobicity" (Cardew *et al.,* 1998).

A study of eight types of membrane with the same cut-off but different materials was conducted by Jonsson *et al.* (1995) with using a low-molecular weight hydrophobic solute (octanoic acid) as foulant to observe the performance of hydrophobic and hydrophilic membrane. As a result, the performance of hydrophilic membrane was better than that of hydrophobic membrane. Chang *et al.* (1999) have mentioned to the effect of this interaction mentioned above against membrane fouling in which the membrane fouling is easer deposited to the hydrophobic membrane than the hydrophilic membrane. On the other hands, the hydrophobic-hydrophobic interactions, between solutes, colloids, microbial cells and membrane, are one of the main causes effecting to membrane fouling tendency in membrane bioreactor system using hydrophobic membrane.

To determine the hydrophilic/hydrophobic characteristic of a certain membrane, a definition of contact angle was proposed. Contact angle is formed by the solid-liquid contacting interface. With the very hydrophilic membrane, the droplet is very attractable to contact with membrane surface and the contact angle is close to 0^{o}. When the contact angle is higher than 90^{o}, the membrane is considered as a hydrophobic membrane. Table 2.3 shows the contact angle of various membrane materials used in MBRs in some previous studies.

Table 2.3 Contact angle of various membrane materials used in MBRs

Polymer	Pore size (μm)	Contact angle (degree)
Polypropylene	-	83[(a)]
Polysulphone	-	73[(a)]
Polyacrylonitrite	-	53[(a)]
	0.05	4[(b)]
Polyvinylidene Fluoride	0.22	83[(b)]
CA/CN[*]	0.22	19[(b)]
Cellulose acetate	-	60[(a)]
	0.45	<5[(c)]
	0.22	<5[(c)]
	0.45	70[(d)]
Polyethersulfone	0.45	<5[(c)]
	0.22	<5[(c)]
	0.10	<5[((c)]
	0.038	77[(d)]
Mixed ester	0.45	<5[(c)]
	0.22	<5[(c)]
	0.10	<5[(c)]
Polycarbonate	0.4	50.3[(c)]
	0.2	46.4[(c)]
	0.1	60.8[(c)]
Polyamide	0.45	48[(d)]
Cellulose nitrate	0.45	64[(d)]

[(a)] Cardew *et al*., 1998 [(c)] Nadir Dizge *et al*., 2011

[(b)] Claudia Laabs, 2004 [(d)] Mafirad *et al*., 2011

[*]Mixed of cellulose acetate and cellulose nitrate

2.3.2 Effect of extracellulose polymeric substance (EPS)

Extracellulose polymeric substance (EPS) and soluble microbial products (SMP) which were identified as the complex high-molecular weight mixture of polymers in biomass such as activated sludge, biofilm… are the products of cell lysis. There are many different classes of macromolecular substances such as polysaccharides, protein, nucleic acids, lipid existing as the compositions of EPS (Sheng *et al.,* 2010). Basically, EPS can be divided into two sub-classes: bound EPS and soluble EPS (Laspidou *et al.,* 2002). Bound EPS was considered as the substances (sheaths, capsular polymers, attached organic materials) bound with the cells, whilst soluble EPS is in the solution or weakly bound with the cells. Figure 2.3 illustrates the definition of bound EPS and soluble EPS. Soluble EPS was mentioned as the different name of SMP (Laspidou *et al*., 2002).

EPS plays an important part in the formation of membrane fouling. It was identified as the most significant factor influencing the membrane fouling (Chang *et al*., 2002). In which, bound EPS have a stronger potential of fouling than other (Wang *et al.,* 2009). Due to the importance of EPS in membrane fouling formation, many studies have focused on the characterization of EPS (Wang *et al.,* 2009; Laspidou *et al.,* 2002; Chang *et al.,* 1999). As a result, it was concluded that the major components of EPS are protein and polysaccharide. Therefore, to study EPS and its influence to membrane fouling, protein and polysaccharide characterizations were used.

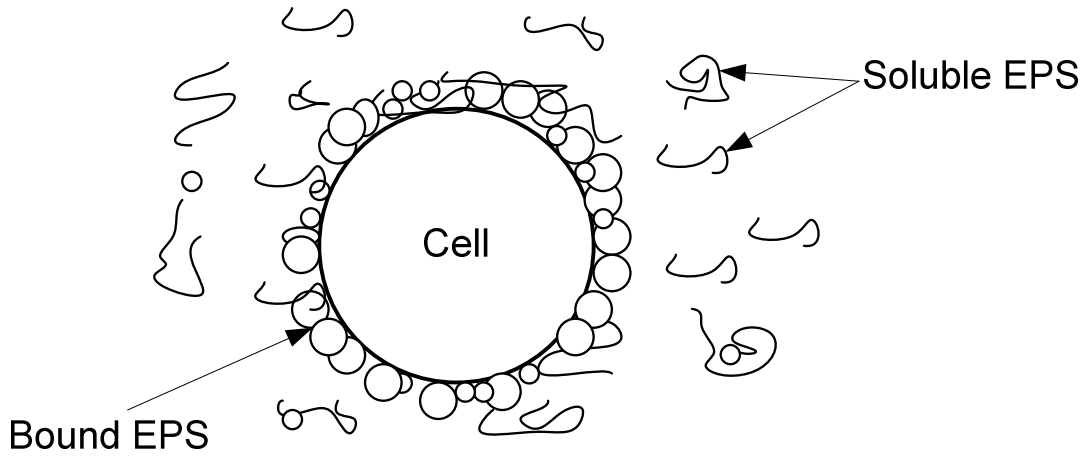

Figure 2.3 Definition of bound EPS and soluble EPS

2.3.3 Effect of mixed liquor suspended solid (MLSS)

Mixed liquor suspended solid (MLSS) was considered as an important factor in treating wastewater in MBRs. However, the relationship between MLSS and fouling is quite complex when focusing on the effect of MLSS concentration to the membrane fouling formation (Judd, 2006). The significant impact of MLSS to membrane fouling was revealed by Le-Clech et al. (2006) with the concentration lower than 5,000 mg/l. While for the MLSS level in the range of 8,000 – 12,000 mg/l, no impact was recorded as the main factors causing membrane fouling. The fouling phenomenon was also observed by conducting an experiment with three levels of MLSS concentration of 6,000 mg/l, 12,000 mg/l and 18,000 mg/l (Brookes *et al*., 2006). The results showed that fouling has just been affected at the lowest concentration and no evident effect at higher MLSS concentration.

Chapter 3

Materials and methods

3.1 Materials

3.1.1 Membrane bioreactor

An experimental MBRs system was operated in this study with the synthesized wastewater. Figure 3.1 shows a schematic of membrane bioreactors. A 30-liter MBR was designed to conduct this experiment, with the submerged flat-sheet module supplied by King Membrane Company in Taiwan.

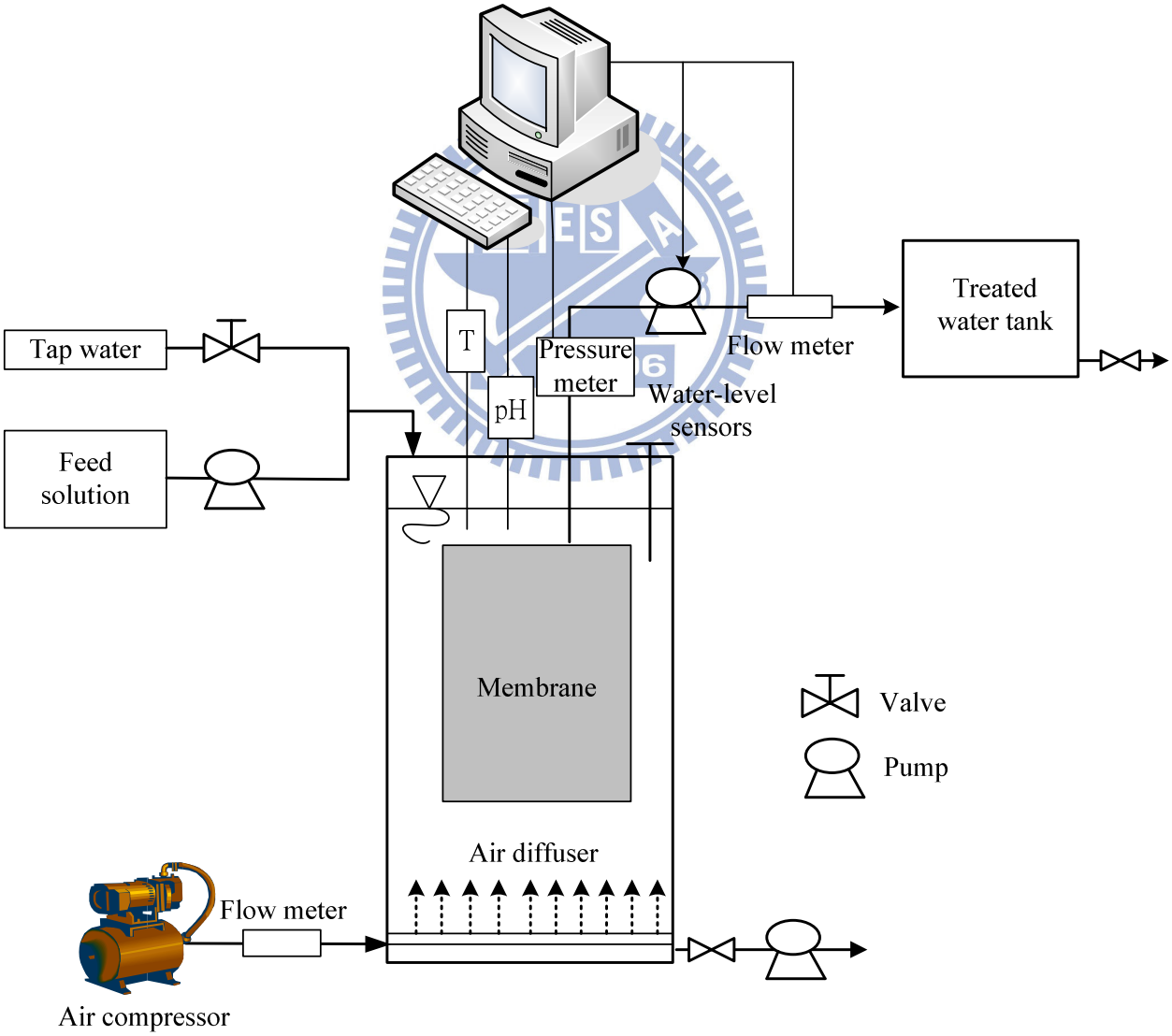

Figure 3.1 Schematic of the MBR system in this study

In order to keep an imposed flux as constant and to control this MBR system conveniently, an automatic control system was also designed and adjusted by ADAMview software. When the system was operating, a feedback of flow-rate signal was transferred from the flow meter to computer and the pump speed increased or decreased to adjust the flow-rate as constant as designed. Feed solution was continuously pumped into the bioreactors from a 60-liter feed solution tank. Water level of the bioreactor was controlled by using the water-level sensors in which the signal from sensors was transferred to the computer and the tap water was pumped into the bioreactor to keep the water level sustainable. Hydrochloric acid was automatically added to adjust the pH of activated sludge from 6.5 to 7.5 in order to make a sustainable environment for the microorganisms living. Air was also continuously supplied from the bottom of the tank through air diffusers below the membrane modules to maintain the aerobic condition. Two bioreactors were maintained with the MLSS concentration lies between 6,000–6,500 mg-MLSS/l and 7,000–7,500 mg-MLSS/l. The average total organic carbon (TOC) of MBRs influent was 160±10 mg/l.

Figure 3.2 Membrane bioreactors

Figure 3.2 shows the real system used in this study. A flux-step method was used to determine critical flux of each membrane type in each reactor. After critical fluxes were found, some imposed sub-critical fluxes were specified and were employed with these two types of membranes. During the running of membrane bioreactors, TOC and MLSS have daily been tested as a basic condition of membrane bioreactor running.

Only when the transmembrane pressure of system reached to 40 kPa, membranes were picked up and were pre-treated for the following experiments. A series of experimental equipment and method such as Confocal Laser Scanning Microscopy (CLSM), Excitation-Emission Matrix (EEM), Fourier Transform Infrared spectroscopy (FTIR), particle size distribution and EPS characterization have been used for characterizing the membrane fouling on membrane surface.

In this study, the flat-sheet membranes used were supplied by King Membrane Company. Two polytetrafluoroethylene (PTFE) MF membranes with a mean pore size of 0.5 μm were used. One is hydrophobic membrane and the other one is hydrophilic. The characteristics of applied membrane in this study are shown in Table 3.1.

Table 3.1 Characteristics of applied membrane in this study

Supplier	Membrane type	Material	Pore size (μm)	Hydrophobicity
King Membrane	MF	PTFE	0.5	HPI
King Membrane	MF	PTFE	0.5	HPO

3.1.2 Feed solution

The synthetic wastewater was used to feed the bioreactors, which was prepared every 3 days with the compositions showed in Table 3.2 according to a research of Ng and Hermanowicz (2005). The synthetic wastewater was contained in a 60-L tank at 4°C and continuously mixed to keep the feed solution as fresh as possible. It was supplied for the system by using a peristaltic pump on the influent stream.

Table 3.2 Compositions of feed solution as the synthetic wastewater

Component		Concentration (mg/l)
Organic		
	CH_3COONa	2527
	Corn Starch	150
	Beef extract	250
	NH_4Cl	670
	KH_2PO_4	154
Inorganic		
	$MgSO_4.7H_2O$	355
	$CaCl_2$	73
	$FeSO_4.7H_2O$	87
	$Na_2MoO_4.2H_2O$	0.08
	KI	0.166
Stock solution		
	$CuCl_2.2H_2O$	0.35
	$MnCl_2.4H_2O$	0.63
	$ZnSO_4.7H_2O$	0.66
	$CoCl_2.6H_2O$	0.15
	H_3BO_3	0.124

Source: Ng and Hermanowicz, 2005

3.2 Methods

3.2.1 Flux-step method for determining critical fluxes

The flux-step method has been developed for finding the critical flux in a MBR according to the constant of flux (Le-Clech *et al.,* 2003a). In this experiment, flux was kept at constant for observing the change of transmembrane pressure (TMP). The increase of TMP was considered as the increase of membrane fouling rate. Therefore, It is based on some specific values of some factors related to TMP such as ΔP_0, dP/dt, K and P_{ave} to determine critical flux. Le-Clech also mentioned to the step length and height as the efficient parameter in flux-step experiment in which the best choice of step length lied in the range of 15 – 30 min, the step height was 3 $lm^{-2}h^{-1}$. Figure 3.3 shows a case of using step-flux method in this study for determining critical flux at 15 min of step length and 3 $lm^{-2}h^{-1}$ of step height and the initial flux was set at 6 $lm^{-2}h^{-1}$.

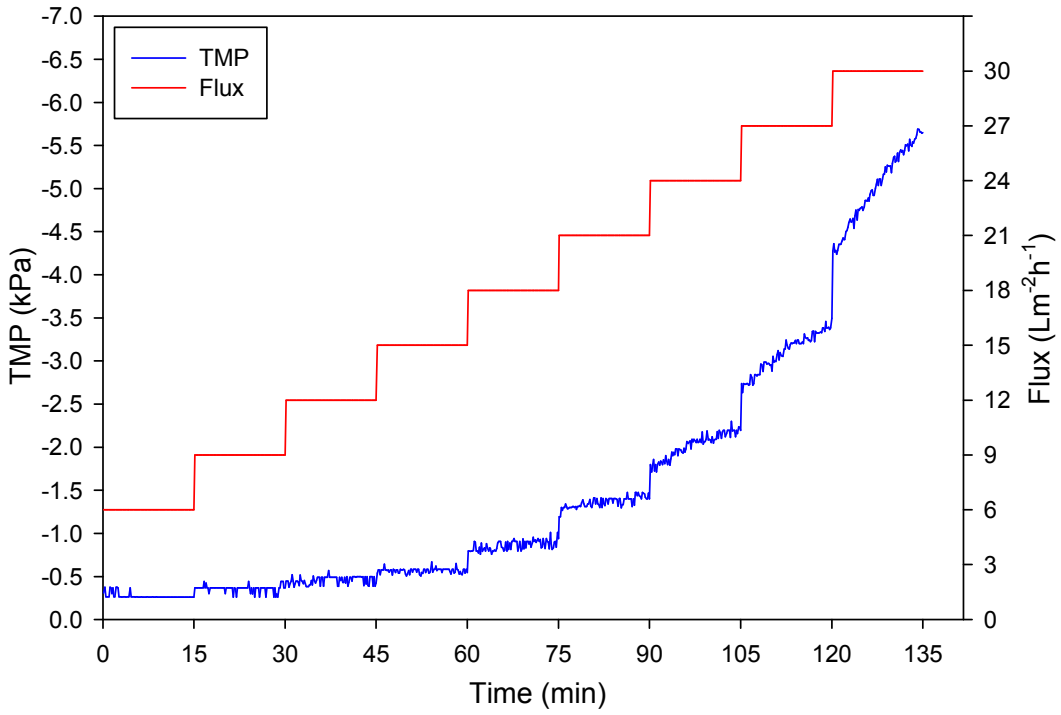

Figure 3.3 Critical flux determinations by flux-step test

A concept of permeability (K) and rate of TMP increase (dP/dt) have been proposed to verify critical flux exactly. A plot of dP/dt and K against flux was generated to determine the critical flux (Le-Clech *et al.,* 2003a; Pollice *et al.,* 2005). These parameters (dP/dt and K) were calculated as these equations below:

$$\frac{dP}{dt} = \frac{TMP_f^n - TMP_i^n}{t_f^n - t_i^n} \quad (3.1)$$

$$K = \frac{J}{P_{ave}} \quad (3.2)$$

$$P_{ave} = \frac{TMP_f^n + TMP_i^n}{2} \quad (3.3)$$

TMP_i^n , TMP_f^n are the initial and final transmembrane pressure (kPa), respectively. J is the arbitrary permeate flux ($lm^{-2}h^{-1}$). t_i^n, t_f^n are the initial and final point time of each step length (s), respectively. P_{ave} is the average pressure of each step length (kPa).

Critical flux is defined as the flux at which $K > 0.9K_0$, where K_0 is the initial permeability measured from the first flux-step (Le-Clech *et al.,* 2003a).

3.2.2 Preparation of fouling sample

The samples for MLSS and TOC analysis were directly taken from the MBRs. Other experiments were done with the samples taken from the fouling layer attached on the membrane at the end of each sub-critical flux operation when the TMP reached to 40 kPa. This sampling procedure was shown in Figure 3.4. After the flat-sheet membrane was removed out of the bioreactor, a hard sheet was intermediately used to scrape off the foulants attaching on the membrane surface and simultaneously rinsed into a beaker contained deionized water. The collected sample was fulfilled up to 75 ml by deionized water and was well mixed by a magnetic stirrer.

After the fouling was scraped, the membrane was cut out from the flat-sheet and immersed into a beaker contained 300 – 350 ml of deionized water for sonication for 30 min to extract the small particle deposited into the membrane pore as well as a certain part of membrane fouling layer that couldn't be removed by scraping step. After sonication step, the membrane would be removed out the beaker. Deionized water was added into the beaker for fulfilling the water-level up to 400 ml

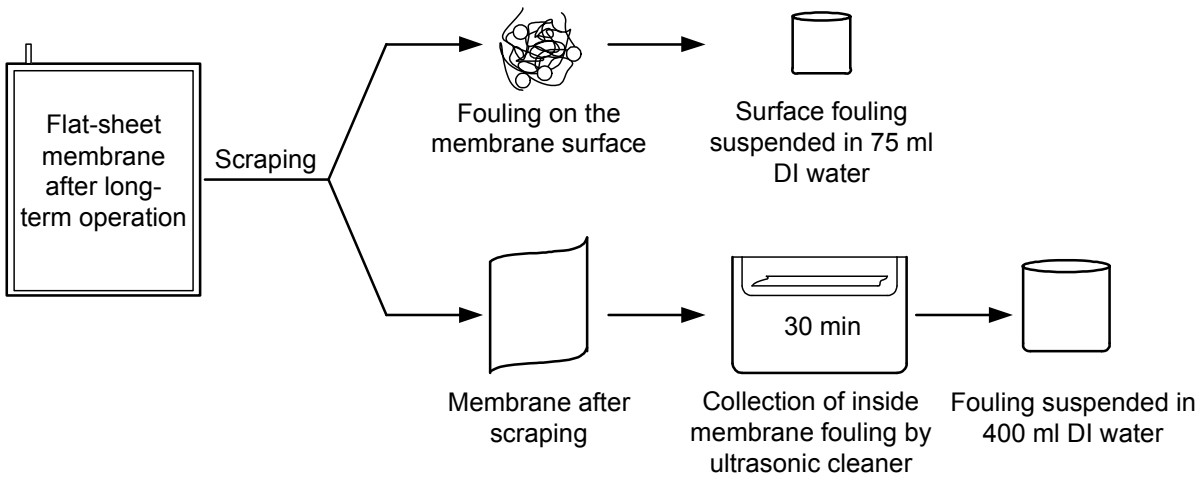

Figure 3.4 Preparation of fouling sample

3.2.3 MLSS and TOC measurement

Analytical method of MLSS bases on the standard methods of American Public Health Association (APHA), 1998. TOC is measured by using a TOC analyzer (TOC-5000A) supplied by the Shimadzu Corporation in Japan. Samples were filtered first by a 0.45 µm membrane filter (Nylon membrane, Millipore Millex-HN). Next, samples were acidified by adding 3-5 drops HCl in order to get rid of inorganic carbon prior to measuring.

3.2.4 Examination of Extracellulose Polymeric Substances (EPS)

3.2.4.1 Extraction of EPS

The purpose of this method is to separate bound EPS and soluble EPS from the sludge solution. This method was applied according to a study of Liu and Fang (2002) about using formaldehyde-NaOH method to extract EPS. EPS extraction from activated sludge sampled from MBRs was clearly illustrated in Figure 3.5. Firstly, 10 ml sludge was centrifuged (U-320R Boeco, Germany) at 4,000 rpm, at 4^{o}C for 20 min to separate the sludge solution into liquid part and solid part. The liquid was filtered through 0.45 µm membrane to obtain soluble EPS. De-ion water was filled up to 10 ml to re-suspend the solid part. Then, 0.06 ml formaldehyde (36.5%) was added in to the samples and kept it at 4^{o}C for 60 min in order to fix the cell by preventing the cell lysis. Next, 4 ml of 1 N NaOH was added into the suspension to increase pH, resulting in the dissociation of acidic group in EPS. This suspension was refrigerated at 4^{o}C for 180 min. The samples then

would be centrifuged at 20,000 G at 4°C for 20 min and be filtrated by 0.2 μm membrane to remove the microbial cells. Bound EPS was obtained after purified by 3,500 Da of dialysis membrane at 4°C for 2 day to remove the extractant residues in the solution.

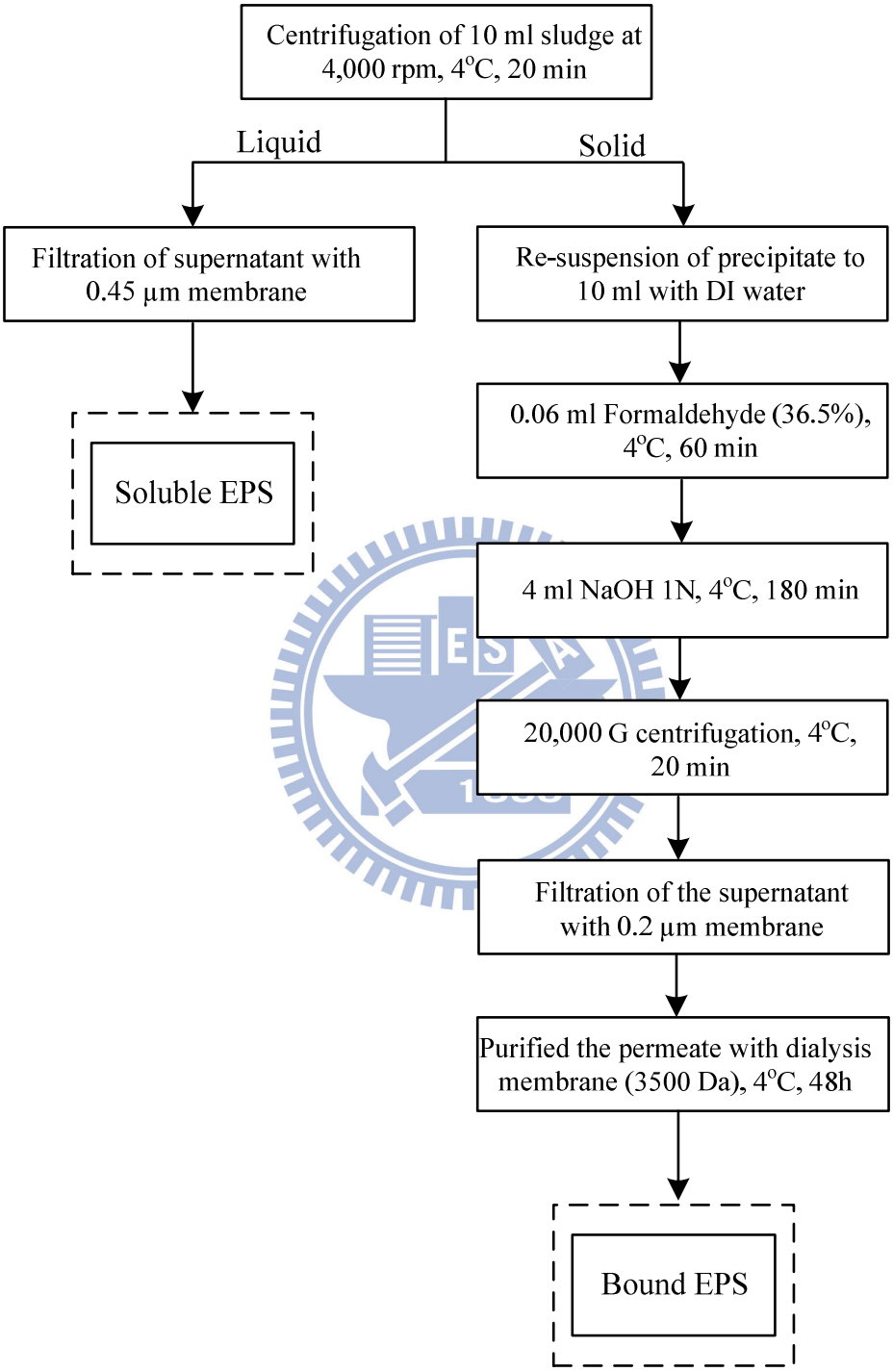

Figure 3.5 Extraction of EPS from activated sludge in MBRs

3.2.4.2 EPS determination

(a) Polysaccharide measurement

This analysis was used to detect and calculate the concentration of polysaccharide in the solution. It was first established by Dubois et al (1956) and was also known as name of phenol-sulfuric acid method. Procedure of polysaccharide measurement was shown as in Figure 3.6. A tube of 1 ml sample was prepared first. Then, 1 ml phenol 5% was added into for separating most sugars existing in the sample. The next step was that adding 5 ml sulfuric acid 75% into the mixture to remove residual phenol. Let the tube stand for 10 min and water bath at 25°C for 15 min for completely reacting. The calibration curve was plotted according to the given glucose concentration 5, 10, 20, 40, 80 mg/l, respectively. The samples were read at 488 nm of wavelength.

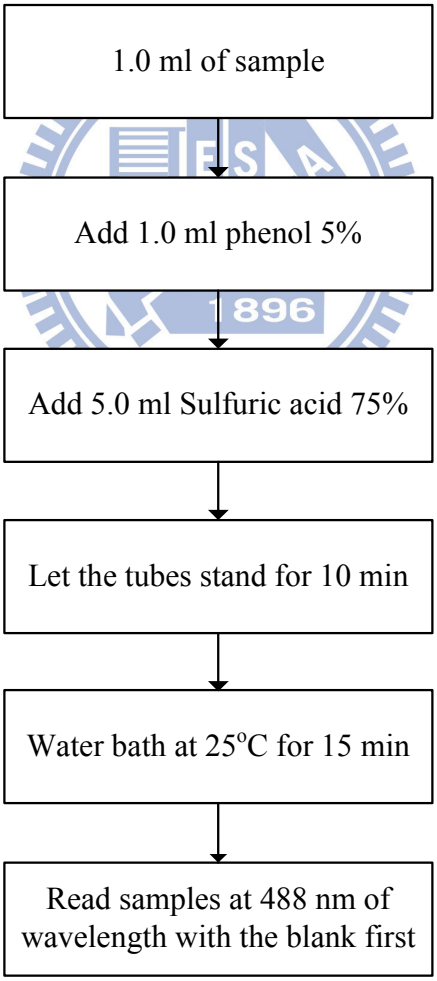

Figure 3.6 Phenol-Sulfuric acid methods for polysaccharide measurement

(b) Protein measurement

To determine the concentration of protein in the solution, a protein determination method was applied following the method of Bradford (1976). Figure 3.7 presents the protein measurement procedures. Figure 3.7a was used when the protein concentration is in the range of 0.1 – 1 mg/ml. A calibration curve was prepared by using Bovine Serum Albumin (BSA) as protein standard.

A tube with 0.1 ml sample was prepared for the experiment. Then, 3 ml Bradford reagent was added to dye protein in the solution. The tube would be rapid mixed at ambient temperature for 5 to 45 min. The absorption of dye is from 365 to 595 nm and the 595 nm of wavelength has been used for measuring protein. In case of the protein concentration is less than 0.1 mg/ml, a procedure in Figure 3.7b is applied with the given calibration curve from 1 to 10 µg/ml.

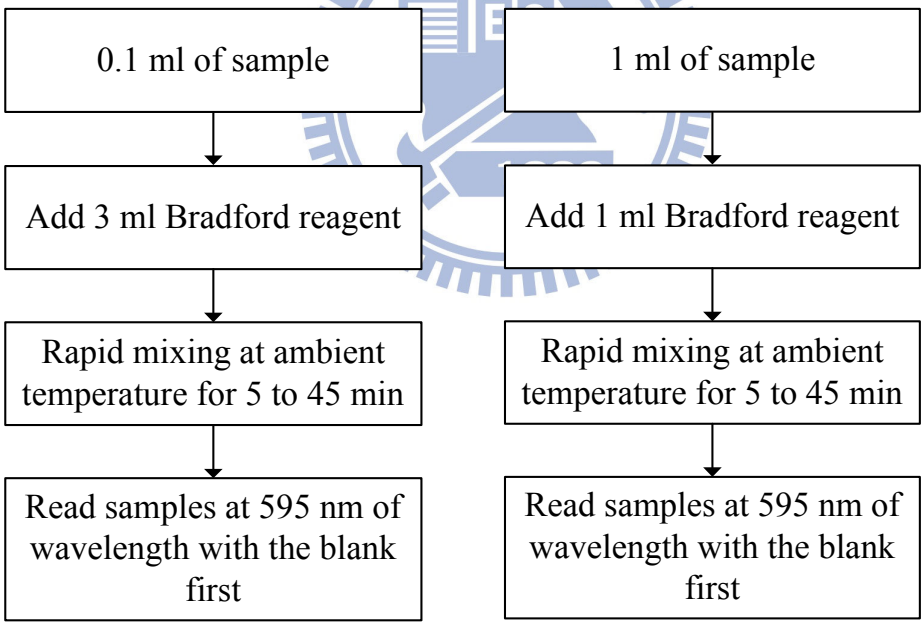

(a) (b)

Figure 3.7 Bradford methods for protein measurement

(a) Protein measurement in range of 0.1-10 mg/ml

(b) Protein measurement in range of 1-10 µg/ml

3.2.5 Confocal Laser Scanning Spectroscopy (CLSM)

The purpose of using CLSM (Leica TCS SP2 Confocal Spectral Microscope Image System, Germany) was to investigate the membrane fouling compositions inside of the membrane fouling layer which were considered as protein and polysaccharides (more details in section 2.3.2).

Protein, nucleic acid (DNA), α-D-glucopyranose polysaccharides and β-D-glucopyranose polysaccharides were stained for CLSM experiment according to a research of Chen et al., (2006). Specimens used in this measurement were prepared as a procedure showed in Figure 3.4. Four types of dyes used to stain protein, nucleic acids (DNA), α-D-glucopyranose polysaccharides and β-D-glucopyranose polysaccharides are Fluorescein isothiocyanate (FITC) (Molecular Probes, USA), Red Fluorescent Nucleic Acid Stains (SYTO 63) (Molecular Probes, USA), Concanavalin A (ConA) (Molecular Probes, USA) and Fluorescent Brightener 28 (Calcoflour white, CW) (Sigma), respectively. Table 3.3 shows a summary of dyes with the given concentration used to stain targets in this experiment and the appropriate excitation-emission wavelength of CLSM for detecting the presence of the stained targets in the specimens.

The staining steps for CLSM were presented in Figure 3.8. A membrane sample was immediately taken from the membrane flat-sheet after removed out of MBR. It was primarily washed by deionized water to remove the unnecessary substances from the membrane surface. Next, some drops of SYTO 63 with 10 μM concentration were first dripped onto membrane sample surface to stain DNA for 30 min. Then, Phosphate buffer saline (PBS) (Amresco, Canada) was used to clean the residues stain from the sample. This step was performed five times before a new stain was added. Protein molecule stained by SYTO 63 was detected by CLSM via 633 nm of excitation wavelength and 650 – 700 nm of emission wavelength. The next step is that 0.1 N $NaHCO_3$ was added prior to FITC staining step to accelerate the efficiency of FITC staining. FITC was used to stain protein with 60 min waiting. FITC was determined via excitation at 488 nm and emission wavelength at 500 – 550 nm. The sample was washed again by PBS. ConA with the excitation-emission range of 543/ 550 – 590 nm was applied to determine the presence of α-D-glucopyranose polysaccharides for 30 min waiting. After washing by PBS, β-D-glucopyranose polysaccharides were stained by CW on the basis of excitation of 400 nm

and emission at 410 – 418 for 30 min. The sample was washed again to remove all the residue stains on the sample surface. Finally, the sample was stick onto the microscope slide for CLSM analysis.

Table 3.3 Summary of dyes with the applied concentration, staining targets, excitation-emission wavelength and indicated color

Dye	Conc.	Target	Excitation (nm)	Emission (nm)	Indicated color
FITC	5 mg/ml	Protein	488	500 – 550	Green
SYTO 63	10 μM	DNA	633	650 – 700	Red
ConA	2.5 mg/ml	α-D-glucopyranose polysaccharides	543	550 – 590	Cyan
CW	5 mg/ml	β-D-glucopyranose polysaccharides	400	410 – 418	Blue

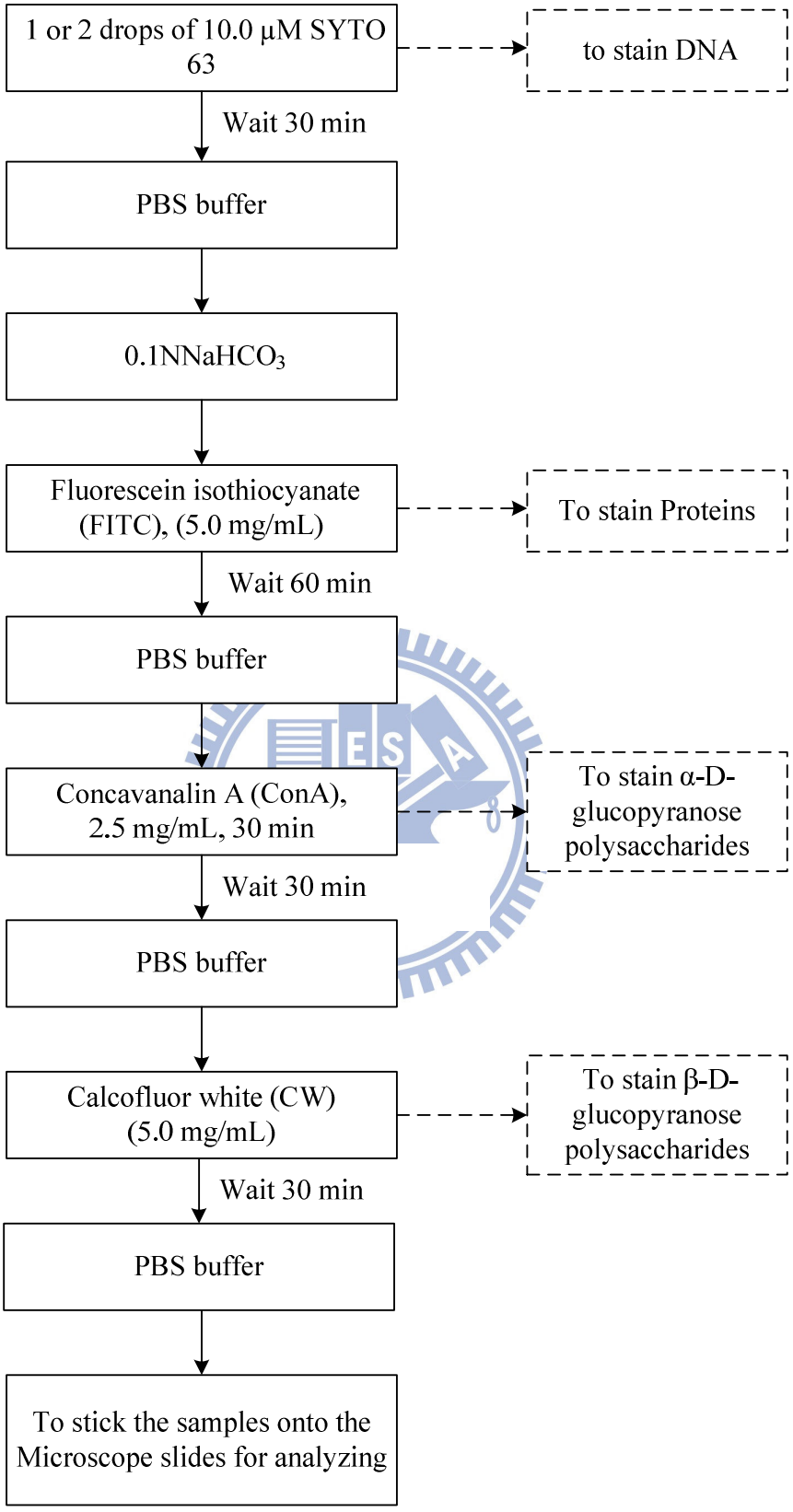

Figure 3.8 Procedure of DNA, protein and polysaccharides staining

3.2.6 Fourier Transform Infrared (FTIR) Spectrophotometer

Fourier Transform Infrared (FTIR) spectrophotometer is the most common instrument that a large number of researchers have used to identify the functional groups of such compounds: humic substances, polysaccharide groups, protein group, etc.

Table 3.4 Wave numbers and functional group of humic substances, polysaccharide and protein in FTIR experiment

Bands (cm^{-1})	Functional group
Humic substances:	
3,400-3,300	O-H stretching
	N-H stretching
2,940-2,900	Aliphatic C-H stretching
1,660-1,630	C=O stretching of amide group
1,620-1,600	Aromatic C=C
1,590-1,517	COO^-, N-H deformation
1,460-1,450	Aliphatic C-H
1,400-1,390	OH deformation, C-O stretching of phenolic OH
1,280-1,200	C-O stretching, OH deformation of COOH
1,170-950	C-O stretching of polysaccharide
Polysaccharides group:	
2,940	Alkane
1,370	Starch
1,170	Tertiary alcohol
1,120	Secondary alcohol
1,040	Aliphatic ether
1,000	Primary alcohol
775	Ethyl
Proteins group	
3,300	Alcohol
1,640	Alkene in aromatic
1,540	Mono substituted amide

Source: Zurasilam et al, 2006

In this study, Attenuated total reflectance-FTIR (ATR-FTIR) (Bomem DA 8.3, Canada) was used to analyze the organic functional groups of foulants on the membrane surface. Samples were prepared from the membrane used in sub-critical flux processes. Samples were dried prior to the analytical performance. FTIR was set to scan from 4000 to 620 cm^{-1} with the resolution of 4 cm^{-1}. Table 3.4 was adopted from a study of Zurasilam *et al* (2006). This table shows the range of wavenumber corresponding with the specific functional groups.

3.2.7 Excitation-Emission Matrix (EEM) method

Excitation-Emission Matrix (EEM) method was used to characterize the fluorescent substance in the membrane fouling including the cake layer deposited on membrane surface and small particle absorbed into the membrane pore. This method can be used to identify many kinds of protein as well as humic acid-like and fulvic acid –like but polysaccharide-like substances can not be detected by this method. Figure 3.9 shows the location of EEM peak based on excitation-emission wavelength. The specific details about excitation-emission wavelength was also showed in Table 3.5

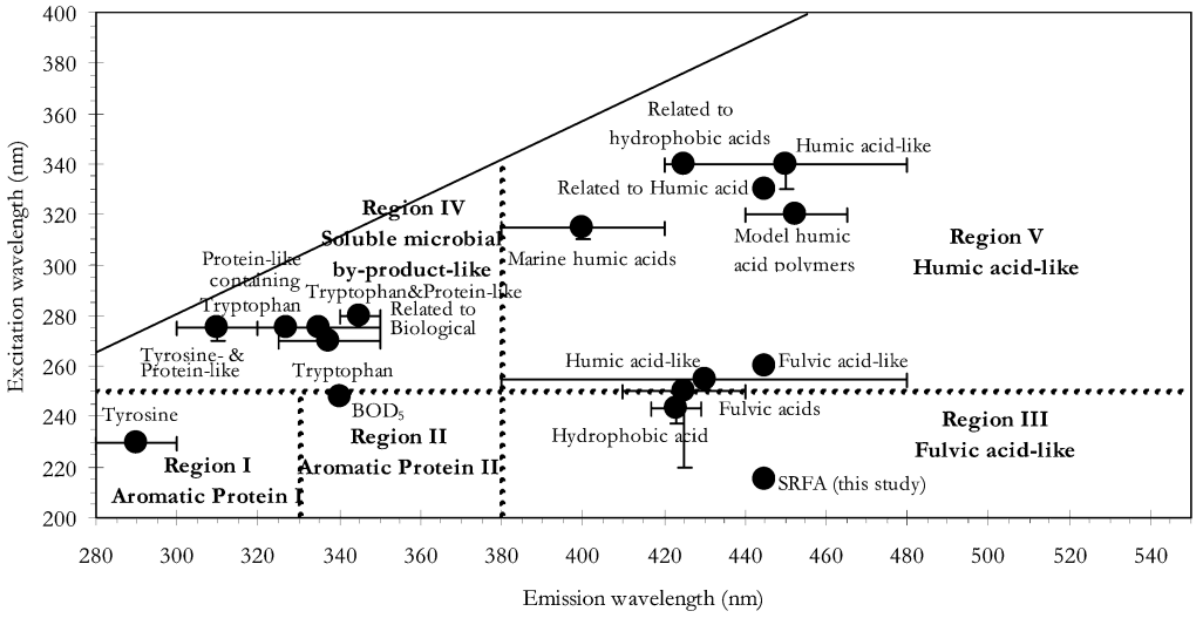

Figure 3.9 Location of EEM peak based on excitation-emission wavelength

Source: Chen *et al.*, 2003

Table 3.5 Excitation-emission wavelength of the five regions of EEM

Region	Excitation (nm)	Emission (nm)	Description
I	200-250	280-330	Tyrosine-like, Aromatic protein
II	200-250	330-380	Tryptophan-like, Aromatic protein
III	200-250	380-500	Fulvic acid-like
IV	250-400	280-380	Soluble microbial by-product-like
V	250-400	380-500	Humic acid-like

Source: Chen *et al*., 2003

Chapter 4

Results and Discussions

4.1 Critical flux determination

4.1.1 Flux-step tests

Flux-step method was conducted to determine the critical flux of different membranes under different operating conditions, in which the beginning flux at 6 $lm^{-2}h^{-1}$, a step height of 3 $lm^{-2}h^{-1}$ and step length of 15 min were selected. All the parameters such as TMP and flux were automatically recorded by the computer system (as introduced in the section 3.1.1).

The flux-step experiments were divided into two stages with different purposes. In order to determine critical flux, the first stage was conducted from the beginning of experiment up to the 120th minute in case of the HPI membrane in MBR-1 with the flux from 6 to 30 $lm^{-2}h^{-1}$, while for the HPI and HPO membrane in MBR-2, it was from the beginning up to the 210th minute with the flux from 6 to 45 $lm^{-2}h^{-1}$. The second stage was conversely conducted against the first stage to observe effects of shear-stress (discussed further in section 4.1.3) to the foulants during the flux-step experiments as the descending phases. Figure 4.1~3 illustrate the critical flux determination for the HPI membrane under the activated sludge concentration (MBR-1) of 7,000 - 7,500 mg-MLSS/L, and for HPI and HPO membrane under 6,000 - 6,500 mg-MLSS/L (MBR-2), respectively.

From Figure 4.1, the TMP was almost stable when the flux increased from 6 to 18 $lm^{-2}h^{-1}$. At the flux of 21 $lm^{-2}h^{-1}$, a little change of TMP from -1.3 kPa to -1.5 kPa was observed which indicated a growing fouling appeared on the membrane. Fouling mechanism, under low flux, is considered as the absorption of small particle such as solute and colloidal fractions in sludge while flocs deposition is absent under a microscope observation (Chang *et al.,* 2002). The sharp increase of TMP from 24 $lm^{-2}h^{-1}$ showed a large amount of membrane fouling created and therefore indicated the vicinity of the critical flux. This trend of TMP is similar in Figure 4.2-3 in which the sharp increase of TMP was observed at a flux of 33 $lm^{-2}h^{-1}$.

Comparisons in changes of TMP between HPI membranes operated in MBR-1 and MBR-2 and between HPI and HPO membrane operated in MBR-2 were plotted in Figure 4.4 so that the occurrence of membrane fouling on membranes in flux-step experiments are easily compared.

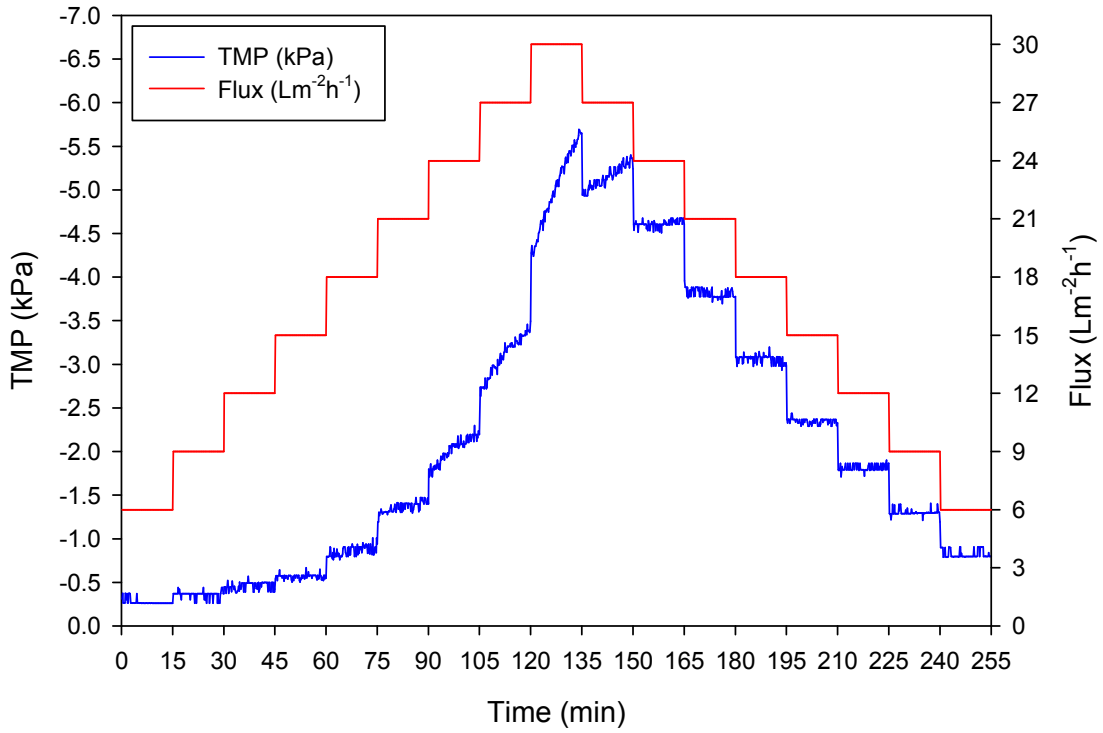

Figure 4.1 Critical flux determination of HPI membrane in MBR-1

The TMP changes of HPI membranes performed in MBR-1 (green curve) and MBR-2 (red curve) give information about the effects of activated sludge characteristics on membrane fouling. Two TMP curves seem to be linear from the flux of 6 - 18 $lm^{-2}h^{-1}$. With the consecutive flux step (from 21 $lm^{-2}h^{-1}$), the TMP line of HPI membrane operated in MBR-1 go dramatically far from the line of HPI membrane operated in MBR-2. The reason for these different trends in TMP changes may be due to the difference of activated sludge concentration. With the concentration 7,000 - 7,500 mg/L, the mixed liquor in MPR-1 would contain a higher amount of colloids, solutes, organic macromolecular such as EPS, SMP or other substances resulting from the cell lysis than that of the 6,000 - 6,500 mg-MLSS/l in MBR-2. Therefore, membranes operating with the higher MLSS concentration are easier to be fouled than those of the lower (Le-Clech *et al.,* 2006).

Regarding to the operation of HPI and HPO membrane in MBR-2, the trends of two TMP curves (red and blue) were quite similar when the flux increased 6 to 27 $lm^{-2}h^{-1}$.

In the next two consecutive flux steps, the TMP of HPI membrane was slightly higher than that of HPO membrane; however, became lower after. In general, this phenomenon means that TMP of the HPI membrane seems to be more sustainable than HPO membrane in the short-term experiments of flux-step method.

Although the changes of TMP can be seen visibly, it is not easy to exactly determine the critical flux value for each case by just observing the TMP changes from these figures. The method to determine critical flux will be described further in section 4.1.2. The flux-step method performance is the first stage of this study, by which critical flux can be found and used for the next tests.

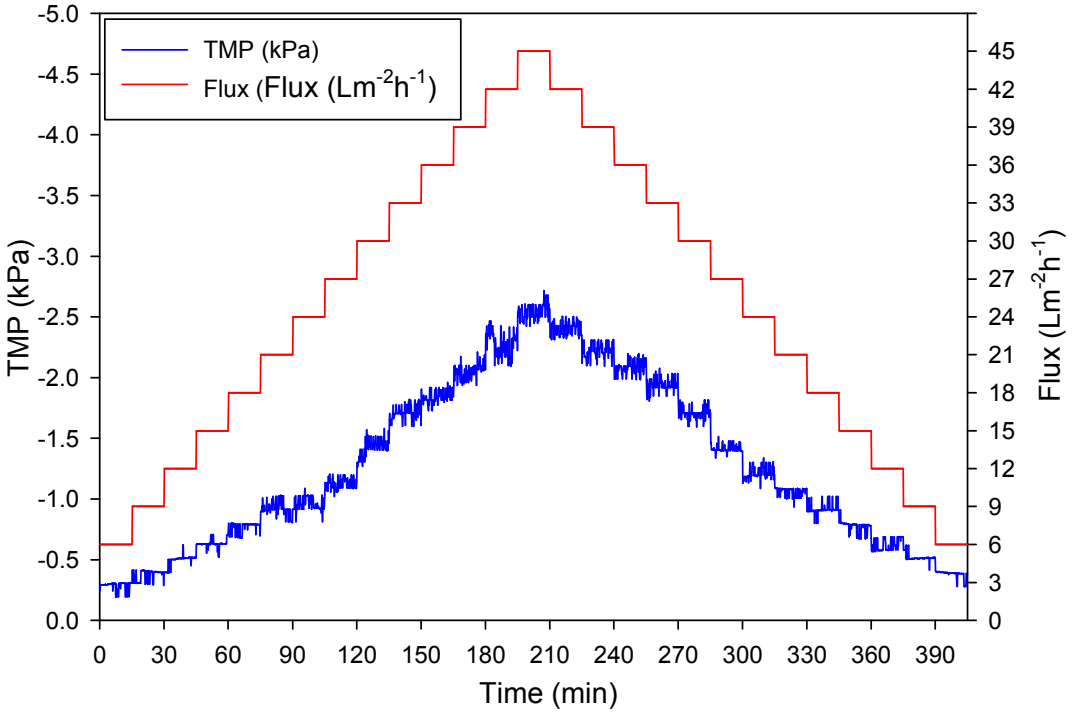

Figure 4.2 Critical flux determination of HPI membrane in MBR-2

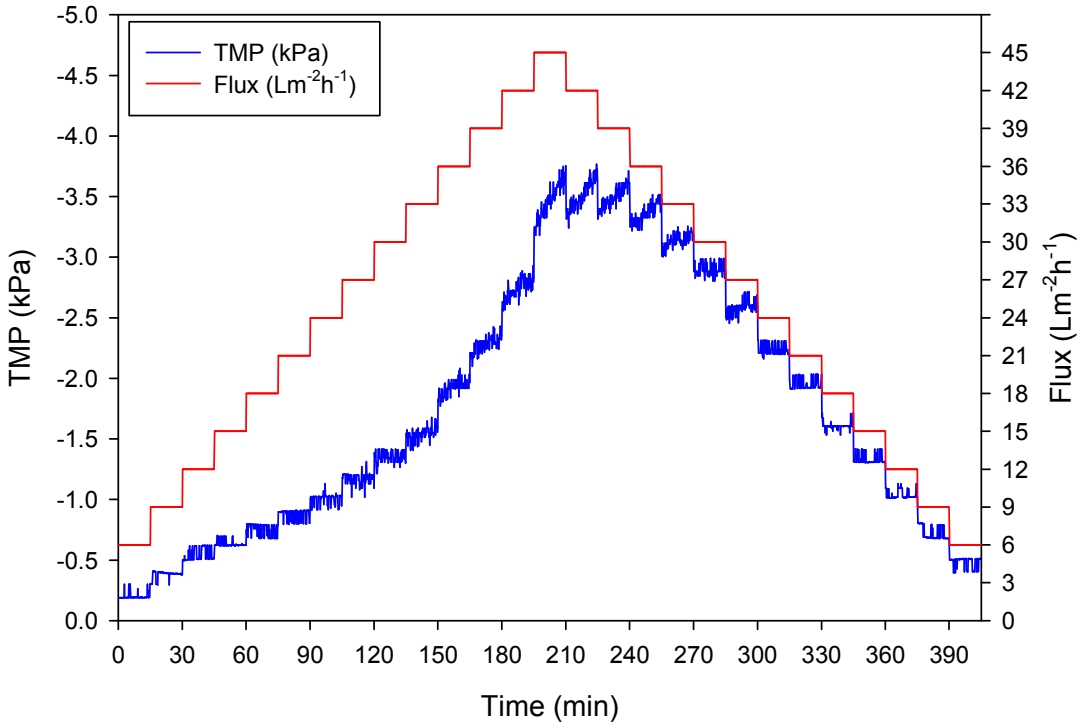

Figure 4.3 Critical flux determination of HPO membrane in MBR-2

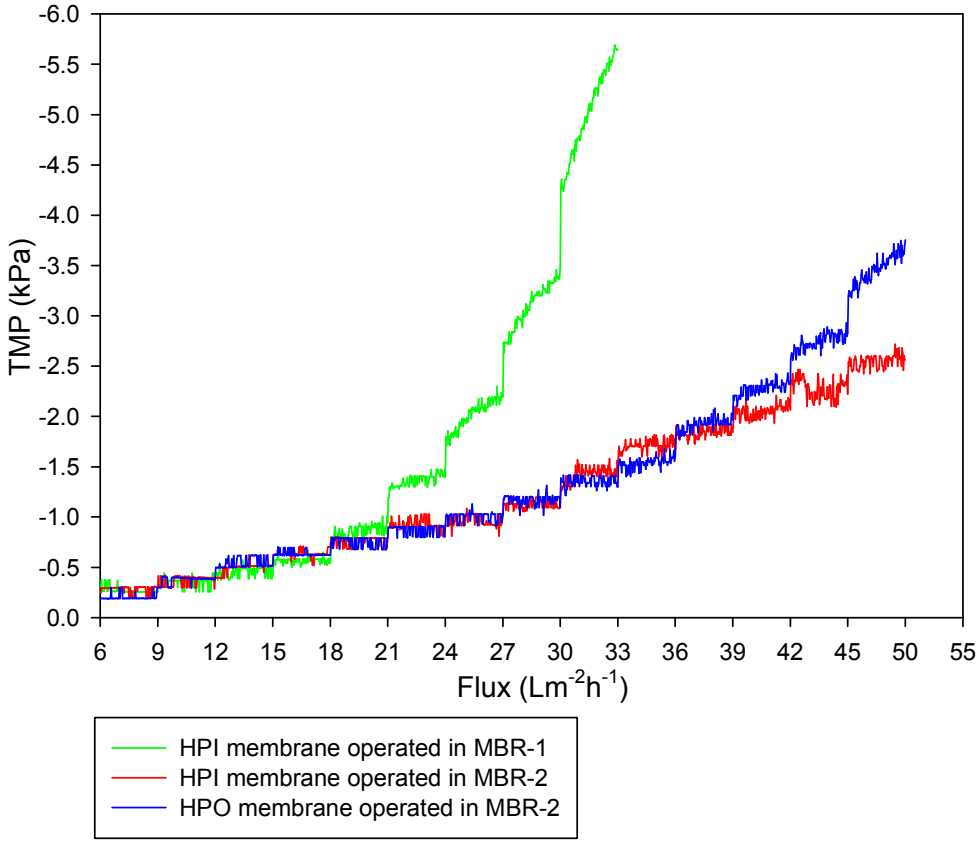

Figure 4.4 Comparison of TMP changes between membranes during flux-step trials

4.1.2 Critical and sub-critical flux determination

In this study, permeability and fouling rate used in critical flux finding were based on an assumption of Le-Clech (2003b). Permeability indicates a quality of membrane that allows the clean water pass through membrane. A decline of permeability shows the appearance of membrane fouling preventing the efficient performance of MBRs. The decrease of membrane permeability is corresponding with the increase of membrane fouling rate.

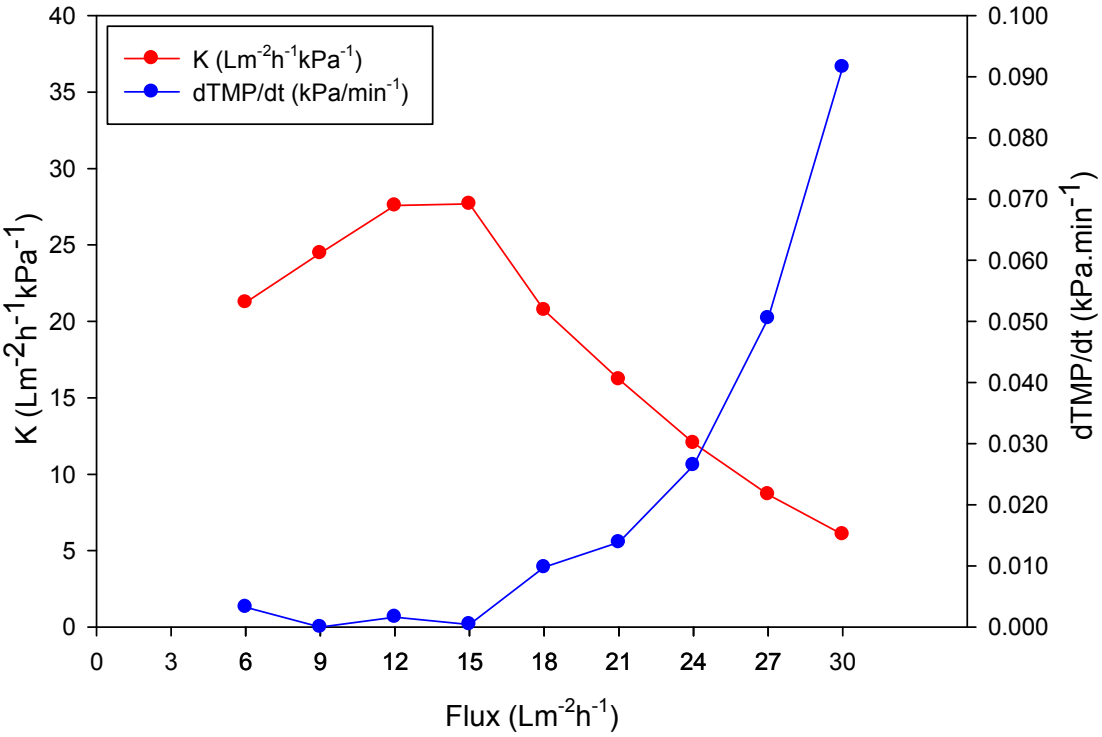

Figure 4.5 Permeability and fouling rate of HPI membrane in MBR-1

A relationship between permeability and fouling rate of HPI membrane in MBR-1, in MBR-2 and HPO membrane in MBR-2 was illustrated in Figures 4.5~7, respectively. In Figure 4.5, permeability increases from 21.2 to 27.7 $lm^{-2}h^{-1}kPa^{-1}$ with the increase of flux from 6 to 15 $lm^{-2}h^{-1}$ (within 3 consecutive flux-steps). Results of unchanged fouling rate (blue curve) showed that membrane fouling in this stage was insignificant. Via flux-step increments from 18 to 30 $lm^{-2}h^{-1}$, the fouling rate then raised together with the reduction of membrane permeability. Figures 4.6~7 show the relationship between permeability and fouling rate of HPI and HPO membrane operated in the same reactor (MBR-2). The permeability of these two cases seems to be more stable than the one in Figure 4.5. In particular, membrane permeability of HPI membrane reached up to 24.7 lm-

$^{2}h^{-1}kPa^{-1}$ after 6 consecutive flux-steps operation, and then it gradually descended. For HPO membrane, the permeability was quite stable for 7 consecutive flux-steps operation before going down.

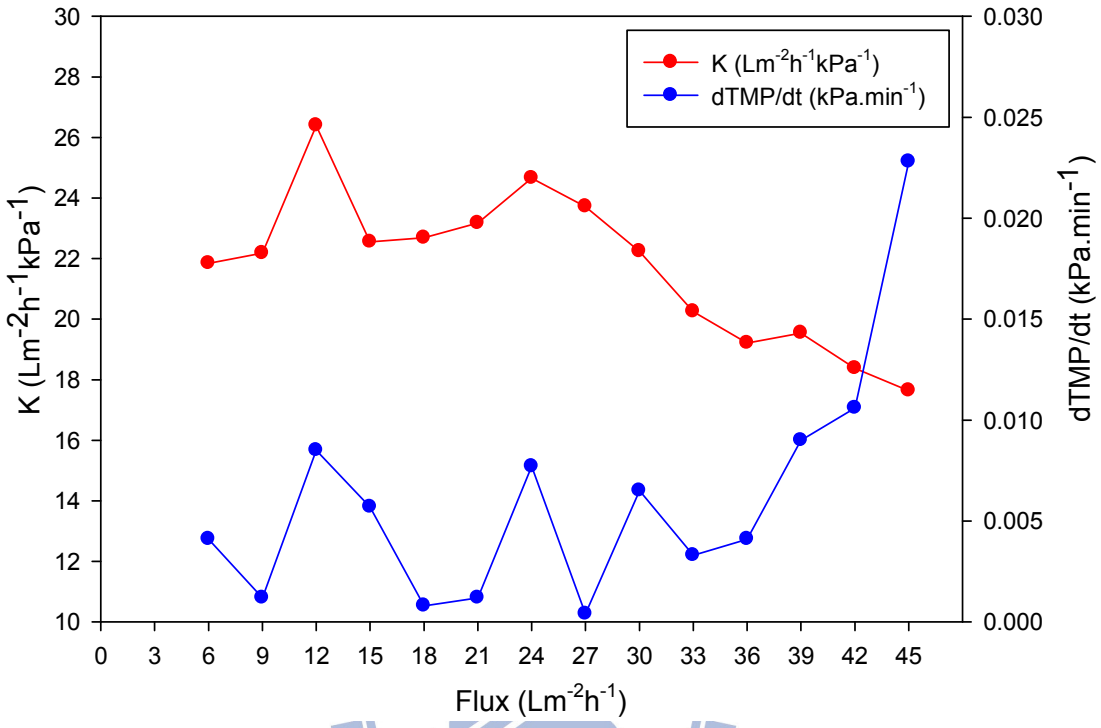

Figure 4.6 Permeability and fouling rate of HPI membrane in MBR-2

The specific data of permeability values and fouling rates are given in Table 4.1. Equation 3.1 was used to calculate the fouling rate and permeability was identified by Equation 3.2~3. In order to determine the exact values of critical fluxes, the initial permeability values were determined. They are 21.2, 21.8 and 21.4 $lm^{-2}h^{-1}kPa^{-1}$ for HPI membrane operated in MBR-1, in MBR-2 and HPO membrane operated in MBR-2. Next, 90% of initial permeability values (K_0) were calculated, as given in Table 4.2, which were used to calculate the sub-critical fluxes.

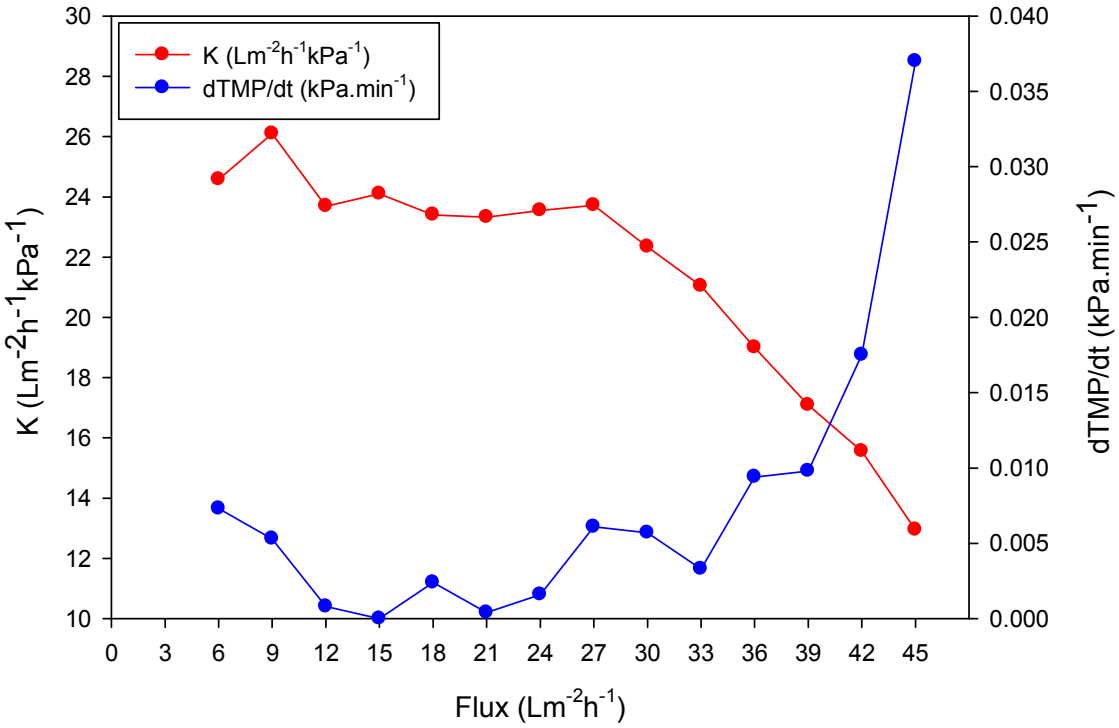

Figure 4.7 Permeability and fouling rate of HPO membrane in MBR-2

Table 4.1 Permeability and fouling rate of HPI and HPO membranes in step-flux experiments

	HPI operated in MBR-1		HPI operated in MBR-2		HPO operated in MBR-2	
Flux ($lm^{-2}h^{-1}$)	**Permeability ($lm^{-2}h^{-1}kPa^{-1}$)**	**Fouling rate ($kPa.min^{-1}$)**	**Permeability ($lm^{-2}h^{-1}kPa^{-1}$)**	**Fouling rate ($kPa.min^{-1}$)**	**Permeability ($lm^{-2}h^{-1}kPa^{-1}$)**	**Fouling rate ($kPa.min^{-1}$)**
6	21.2*	0.0033	21.8*	0.0041	24.6*	0.0073
9	24.5	0.0000	22.2	0.0012	26.1	0.0053
12	27.6	0.0016	26.4	0.0085	23.7	0.0008
15	27.7	0.0004	22.5	0.0057	24.1	0.0000
18	20.7	0.0097	22.7	0.0008	23.4	0.0024
21	16.2	0.0138	23.2	0.0012	23.3	0.0004
24	12.0	0.0265	24.7	0.0077	23.5	0.0016
27	8.7	0.0505	23.7	0.0004	23.7	0.0061
30	6.0	0.0916	22.2	0.0065	22.3	0.0057
33	-	-	20.2	0.0033	21.0	0.0033
36	-	-	19.2	0.0041	19.0	0.0094
39	-	-	19.5	0.0090	17.1	0.0098
42	-	-	19.6	0.0106	15.5	0.0175
45	-	-	18.8	0.0228	12.9	0.0370

(*) K_0 : initial permeability

Table 4.2 Critical flux determination

Membrane	MLSS (mg/l)	90% K_0 ($lm^{-2}h^{-1}kPa^{-1}$)	$K > 90\%K_0$ ($lm^{-2}h^{-1}kPa^{-1}$)	Critical flux ($lm^{-2}h^{-1}$)
HPI	7,000 – 7,500	19.1	20.7	18
HPI	6,000 – 6,500	19.6	20.2	33
HPO	6,000 – 6,500	22.1	22.3	30

4.1.3 Hysteresis loop for the short-term experiment

Hysteresis loop was observed at three above step-flux experiments to assess the stability and reversibility of fouling. In the other word, the effects of shear-stress in MBRs against the formation of fouling were considered.

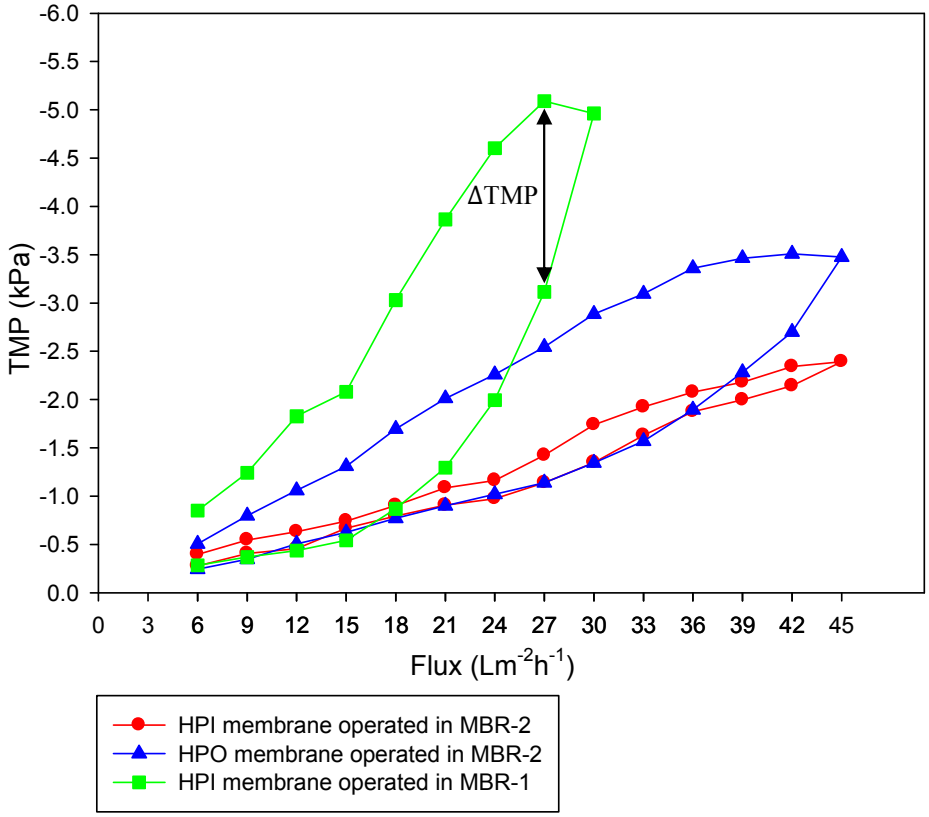

Figure 4.8 Hysteresis loop for the short-term tests

The results in Figure 4.8 point out that the TMP values of all corresponding fluxes obtained from the ascending phase were higher than in the descending phase. This indicates to the occurrence of membrane fouling because the increase in fouling rate was observed as the increase of TMP with a proportional relation. Equation 2.1 can be summarized as following:

$$J = \frac{\Delta P}{\mu R} \rightarrow R = \frac{\Delta P}{\mu J} \qquad (4.1)$$

The viscosity of solution (μ) in the equation was constant and flux (J) was the same in operation. Equation 4.1 clearly depicts the proportional relationship between total resistances (including membrane fouling) with TMP. The uneven of TMP (ΔTMP) between the same flux of hysteresis loop conducted in the ascending phase and descending phase was considered as the amount of fouling formed on the membrane surface. In Figure 4.8, at flux of 18 $lm^{-2}h^{-1}$, we can obviously see the difference about membrane fouling among three hysteresis curves. The ΔTMP of HPI membrane operated in MBR-2 (red curve) is equal to 5.1% of the ΔTMP of HPI membrane operated in MBR-1 (green curve). While for the ΔTMP of HPO membrane operated in MBR-2 (blue curve), it is 43.1%. Moreover, at the initial point as well as the end point of this experiment (J = 6 $lm^{-2}h^{-1}$), it is 19.3% and 47.4% of the ΔTMP of HPI membrane operated in MBR-1 for HPI and HPO membrane in MBR-2, respectively.

Regarding to the removal of fouling by shear-stress, it can be assessed by the disparity of ΔTMP between the flux of 6 and 18 $lm^{-2}h^{-1}$ (other certain flux could be selected for this assessment excluding the initial flux of 6 $lm^{-2}h^{-1}$) in an experiment. In case of HPI membrane operated in MBR-1, the ΔTMP at 6 $lm^{-2}h^{-1}$ was equal to 26.38% of the ΔTMP at 18 $lm^{-2}h^{-1}$. That meant the fouling removal by shear stress was 73.62%. Moreover, this removal was 45.2% for HPO membrane operated in MBR-2 and 0% for HPI membrane operated in MBR-2. In the later case of 0% of fouling removal, this can be explained due to the small amount of fouling absorbed in the inside of the membrane pore causing the uselessness of shear stress.

In conclusion, with the same membrane material, operation in a reactor with higher sludge concentration would cause a higher propensity of membrane fouling. HPO membrane seems to be easier fouled than HPI membrane in the short-term experiment.

4.2 TMP change in sub-critical flux operation

Long-term experiments were conducted to observe the occurrence of membrane fouling under sub-critical flux operation. Figure 4.9 shows the variation of TMP under various sub-critical fluxes. In theoretical point of view, the membrane fouling would not occur under sub-critical flux (Field *et al.,* 1995). But in practice, membrane fouling always occurs even operated under sub-critical flux.

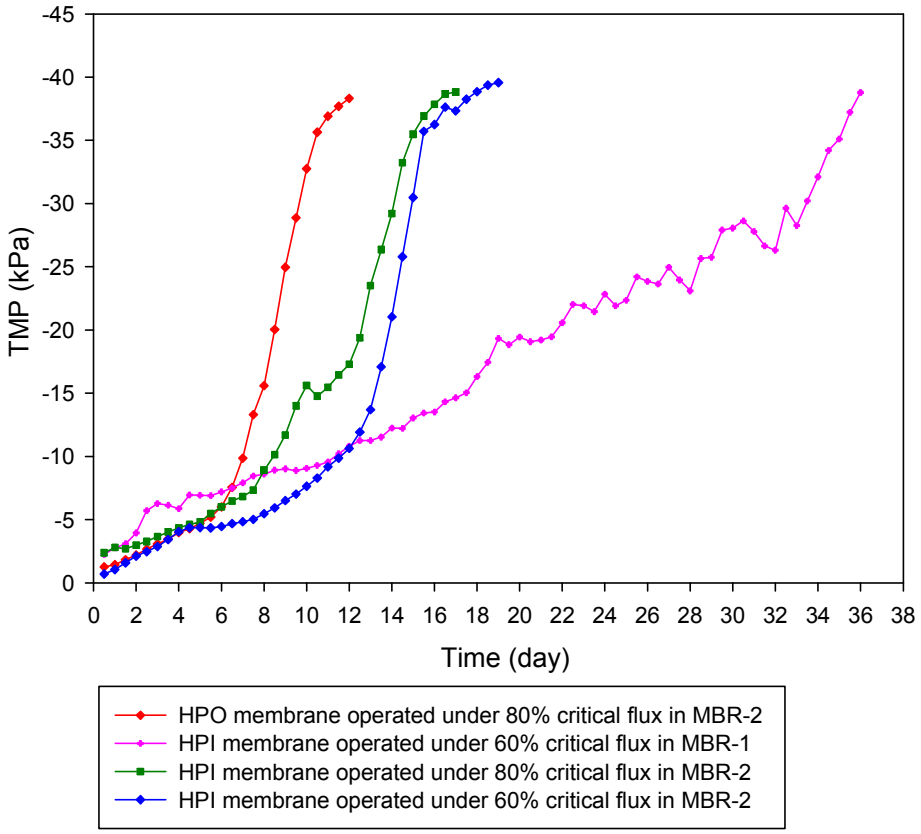

Figure 4.9 Variation of TMP under various sub-critical fluxes operation

In Figure 4.9, the imposed flux was controlled with a given sub-critical flux as calculated in Table 4.2. It is obvious that membrane fouling occurred in the first day of operation. The TMP of HPO membrane operated under 80% critical flux in MBR-2 exhibited the fastest jump up to approximately 40 kPa after 11-days operation. It is 16-days and 18-days operation for HPI membrane operated under 80% and 60% of critical flux in MBR-2, respectively. HPI membrane operated under 60% critical flux in MBR-1 shows the longest operation time, approximately 36 days.

The reason for the fast jump of the red color curve might be due to the hydrophobic interaction between fouling and membrane material. Green and blue color

show a comparison between the same HPI membranes operated under the same operation condition but the flux was different at 60% critical flux and 80% critical flux, respectively. As a result, the higher the flux controlled, the faster the TMP jumped. Figure 4.10 shows the membrane after long-term sub-critical flux operation.

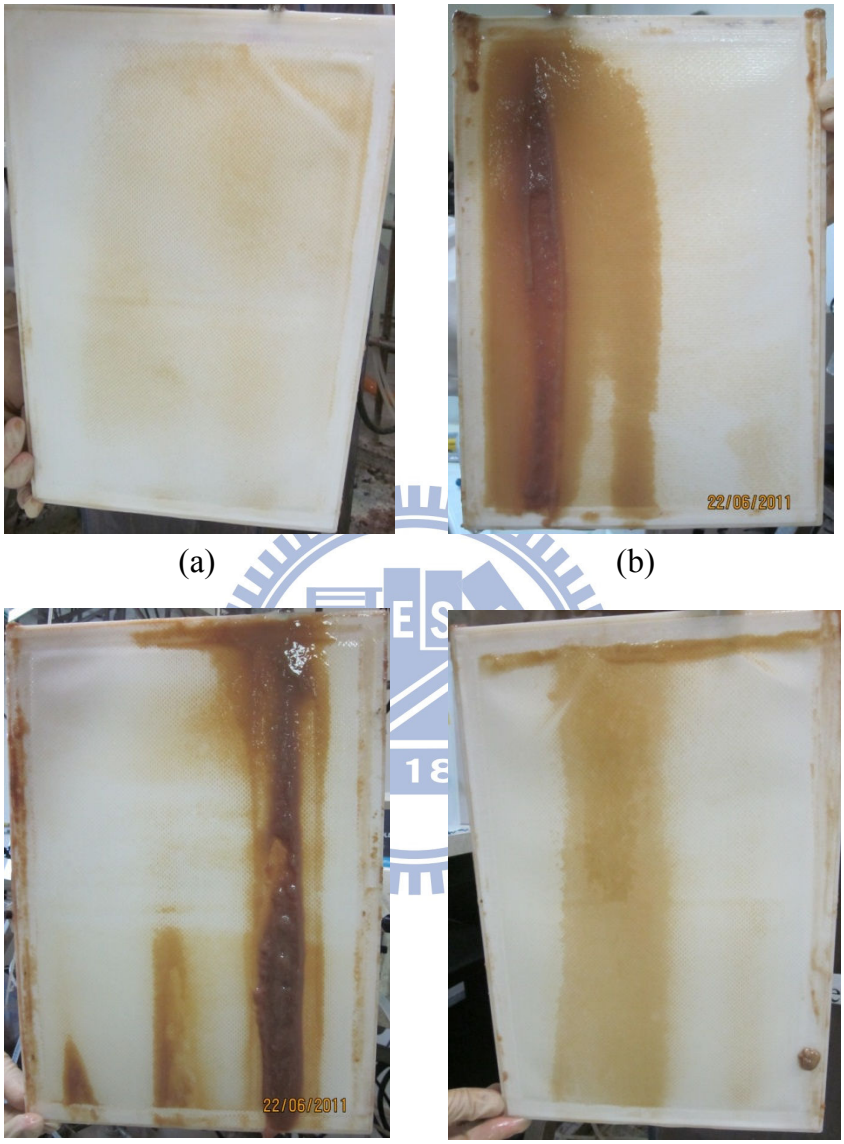

(a) (b)

(c) (d)

Figure 4.10 Flat-sheet membranes after long-term sub-critical fluxes operation

(a) HPO membrane operated under 80% of critical flux in MBR-2

(b) HPI membrane operated under 80% of critical flux in MBR-2

(c) HPI membrane operated under 60% of critical flux in MBR-1

(d) HPI membrane operated under 60% of critical flux in MBR-2

4.3 Membrane performance under different operation condition

The change of MLSS in activated sludge and TOC in permeate were monitored every day to observe the stability of the system. If any trouble occurred in the system, a suitable adjustment should be needed for keeping the MBRs operating under given conditions. Figures 4.11~14 present a fluctuation of MLSS, TOC in permeate and TOC removal from the beginning to the end of operation. The operational conditions seem to be stable and meet the given operation condition shown in scope of study (Figure 1.1). The average MLSS, TOC in permeate and TOC removal were shown in Table 4.3, in which the average MLSS for MBR-1 was 7371 ± 287 mg/l, permeate TOC was 1.80 ± 0.51 mg/l and for TOC removal, it was approximately 98.88%. For MBR-2, all operational case are recorded in Table 4.3

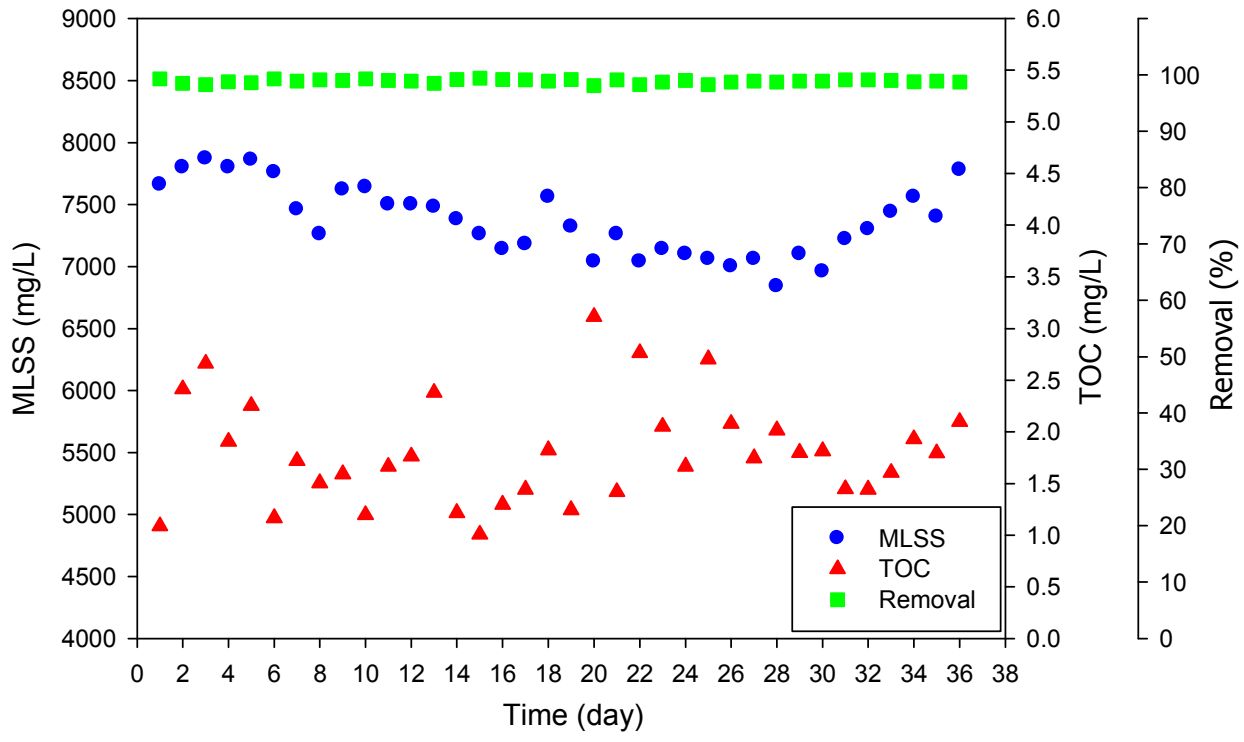

Figure 4.11 Operational conditions of HPI membrane with 60% of critical flux operated in MBR-1

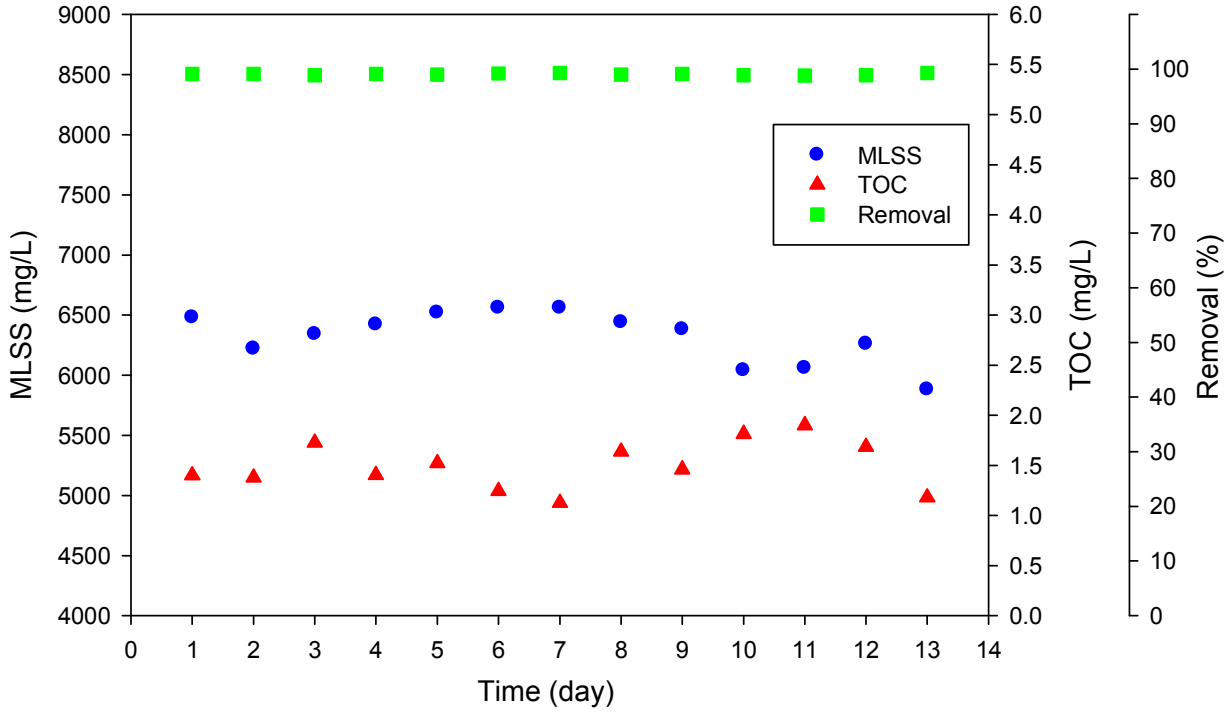

Figure 4.12 Operational conditions of HPO membrane with 80% of critical flux operated in MBR-2

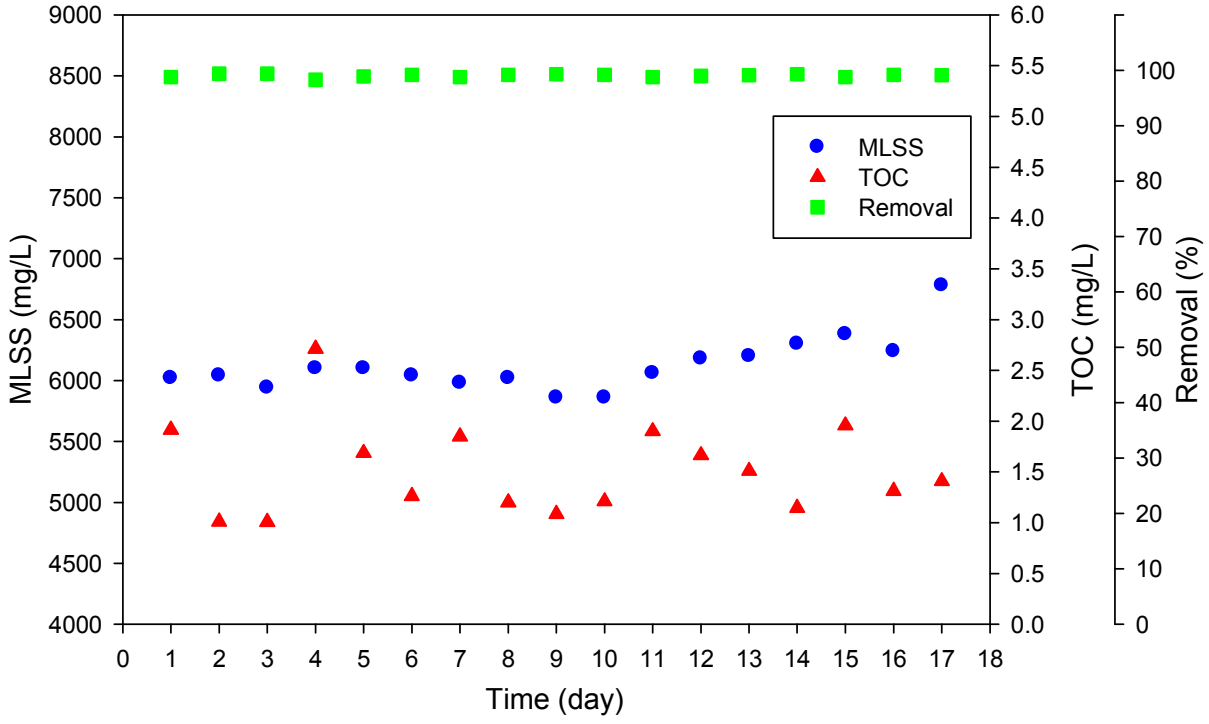

Figure 4.13 Operational conditions of HPI membrane with 80% of critical flux operated in MBR-2

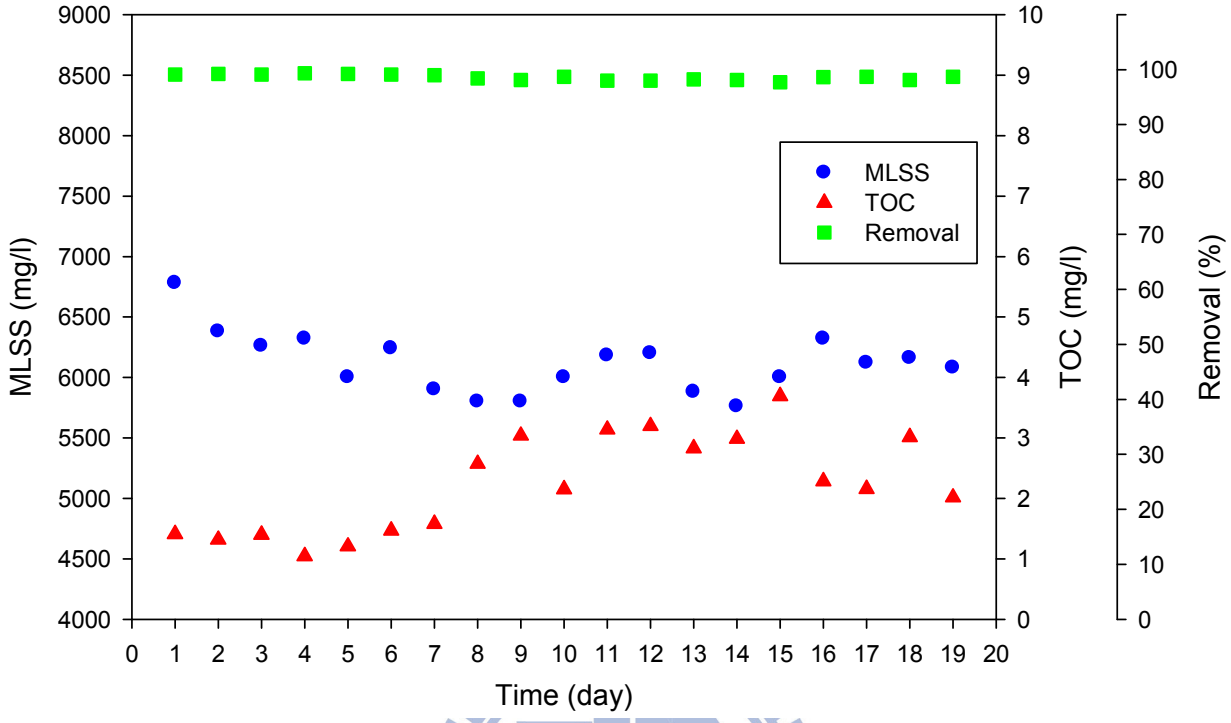

Figure 4.14 Operational conditions of HPI membrane with 60% of critical flux operated in MBR-2

Table 4.3 The average MLSS, TOC in permeate and TOC removal

Membrane	Bioreactor	Percentage of critical flux (%)	MLSS (mg/l)	TOC (mg/l)	TOC removal (%)
HPI	MBR-1	60	7371 ± 287	1.80 ± 0.51	98.88 ± 0.32
HPI	MBR-2	60	6115 ± 249	2.24 ± 0.81	98.59 ± 0.51
HPI	MBR-2	80	6124 ± 221	1.52 ± 0.45	99.05 ± 0.29
HPO	MBR-2	80	6320 ± 216	1.50 ± 0.24	99.05 ± 0.16

4.4 Analysis of membrane fouling

4.4.1 Qualitative analysis of foulant

4.4.1.1 Detection of EPS compositions by FTIR analysis

The FTIR spectra of membrane fouling occurred on HPI and HPO membrane operated under different operational conditions are illustrated in Figure 4.15. The functional groups of foulants were detected at some specific peaks for four cases as introduced above. The peak at wave number of 1035 cm^{-1} shows the presence of polysaccharides (Grube *et al.*, 2006). While at wave number of two peaks near 1639 and 1531 cm^{-1}, that are assigned to the existing of Amide-I and Amide-II represented to the presence of protein in membrane foulants (Wang *et al.*, 2008; Kimura *et al.*, 2005). N-H stretching and C-H stretching was observed at two peaks with the wave number of 3284 and 2920 cm^{-1}, respectively (Zurasilam *et al.*, 2006). As a result, these FTIR experiments have demonstrated to the presence of proteins and polysaccharides in the membrane foulants on membrane surface.

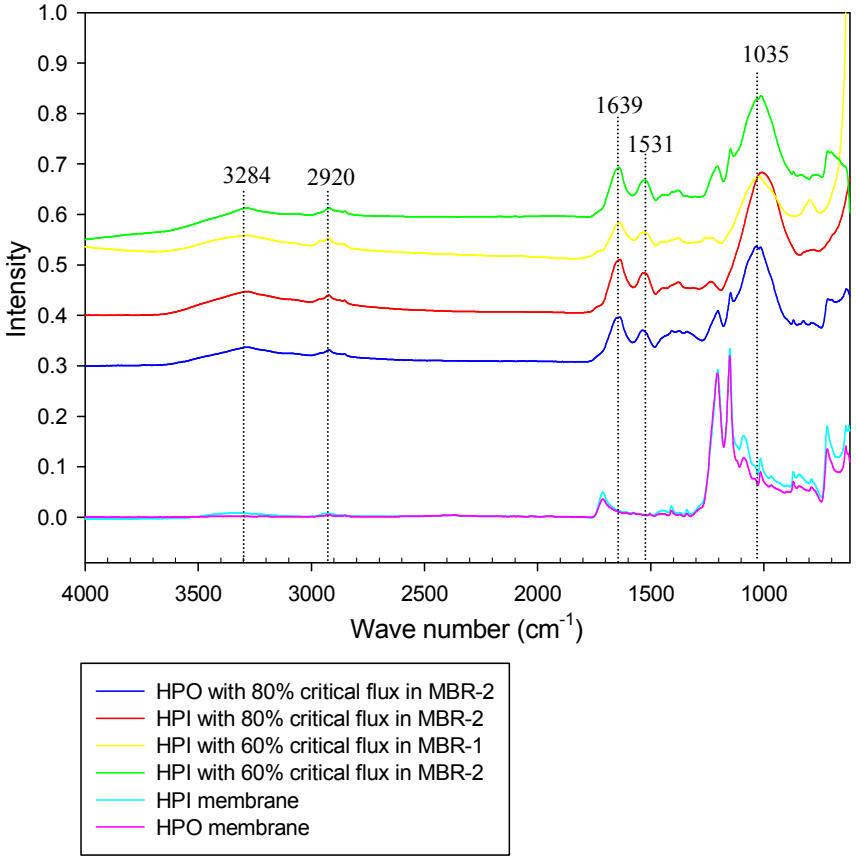

Figure 4.15 FTIR spectra of fouling on membrane surface

4.4.1.2 Protein composition of foulant

The EEM fluorescence spectra of membrane fouling in cake layer and inside of membrane pore operated by four imposed sub-critical fluxes were illustrated in Figures 4.16~19. EEM spectra show information about the fouling compositions by observing the distribution region of it. There are five regions in EEM spectra numbered from Region I to V as clearly introduced in Figure 3.9 and Table 3.5. In the results, it was also numbered for a straightforward assessment about the fouling compositions. All the results with the main peaks just located on Region I and IV. Region I indicate to the tyrosine-like aromatic protein (Chen *et al*, 2003; Wang *et al*, 2009), while Region IV refers to soluble microbial by-product-like protein. That meant protein and protein-like products always existed in the membrane foulants for all operational case.

Table 4.4 shows the peaks location and intensity of membrane fouling as protein. Regarding to the fouling (was assumed as protein including tyrosine-like protein and soluble microbial protein) in cake layer, the fouling formed on HPI membrane surface operated with 60% critical flux in MBR-1 were higher than that in MBR-2 based on the peaks intensity. Proteins on HPI membrane operated with 80% of critical flux in MBR-2 presented the higher concentration of proteins than that of 60% critical flux and it also higher than proteins on HPI membrane.

In case of membrane pore inside, fouling on HPI membrane operated with 60% of critical flux in MBR-1were lower than that in MBR-2. Operated with 80% of critical flux in MBR-2, the proteins in fouling formed on HPI membrane were higher than that operated with 60% of critical flux and also higher than the protein in fouling deposited on HPO membrane surface.

Looking back to see the Figure 4.9, HPO membrane operated under 80% of critical flux in MBR-2 was fouled quicker than HPI membrane illustrated by the quick jump of TMP. But in this section, the fouling (as protein) of HPO membrane presented the lower concentration not only in cake layer but also in membrane pore inside than HPI membrane. That meant proteins didn't play a role in the TMP increasing of HPO compared to HPI membrane.

In contrary, with the difference of imposed flux operation, HPI membrane with 80% of critical flux was fouled quicker than HPI membrane with 60% of critical flux

corresponding with the protein concentration in EEM test. The protein concentration of HPI with 80% of critical flux was higher than that of HPI with 60% of critical flux in two cases: in cake layer and inside of membrane pore.

In case of HPI membrane operated under 60% of critical flux but in different MBR, the results show that, the protein concentration in cake layer of membrane in MBR-1 was relatively higher than in MBR-2, but in membrane pore inside, it was conversely. This reveals that the proteins inside membrane pores effect to the quicker TMP increasing of HPI membrane in MBR-2.

Table 4.4 Peaks location and intensity of membrane fouling compositions

				Region I		Region IV	
	Membrane	**Bioreactor**	**Percentage of critical flux (%)**	**Ex/Em**	**Intensity**	**Ex/Em**	**Intensity**
In cake layer	**HPI**	MBR-1	60	230/320	>1000	270/330	>1000
	HPI	MBR-2	60	230/322	247.3	270/322	317.6
	HPI	MBR-2	80	230/320	>1000	270/330	>1000
	HPO	MBR-2	80	230/322	718.2	280/327	378.5
Inside of membrane pore	**HPI**	MBR-1	60	230/320	211.9	270/322	143.6
	HPI	MBR-2	60	230/322	281.4	270/322	175.1
	HPI	MBR-2	80	230/322	753.1	270/322	753.9
	HPO	MBR-2	80	230/322	315.6	280/326	162.4

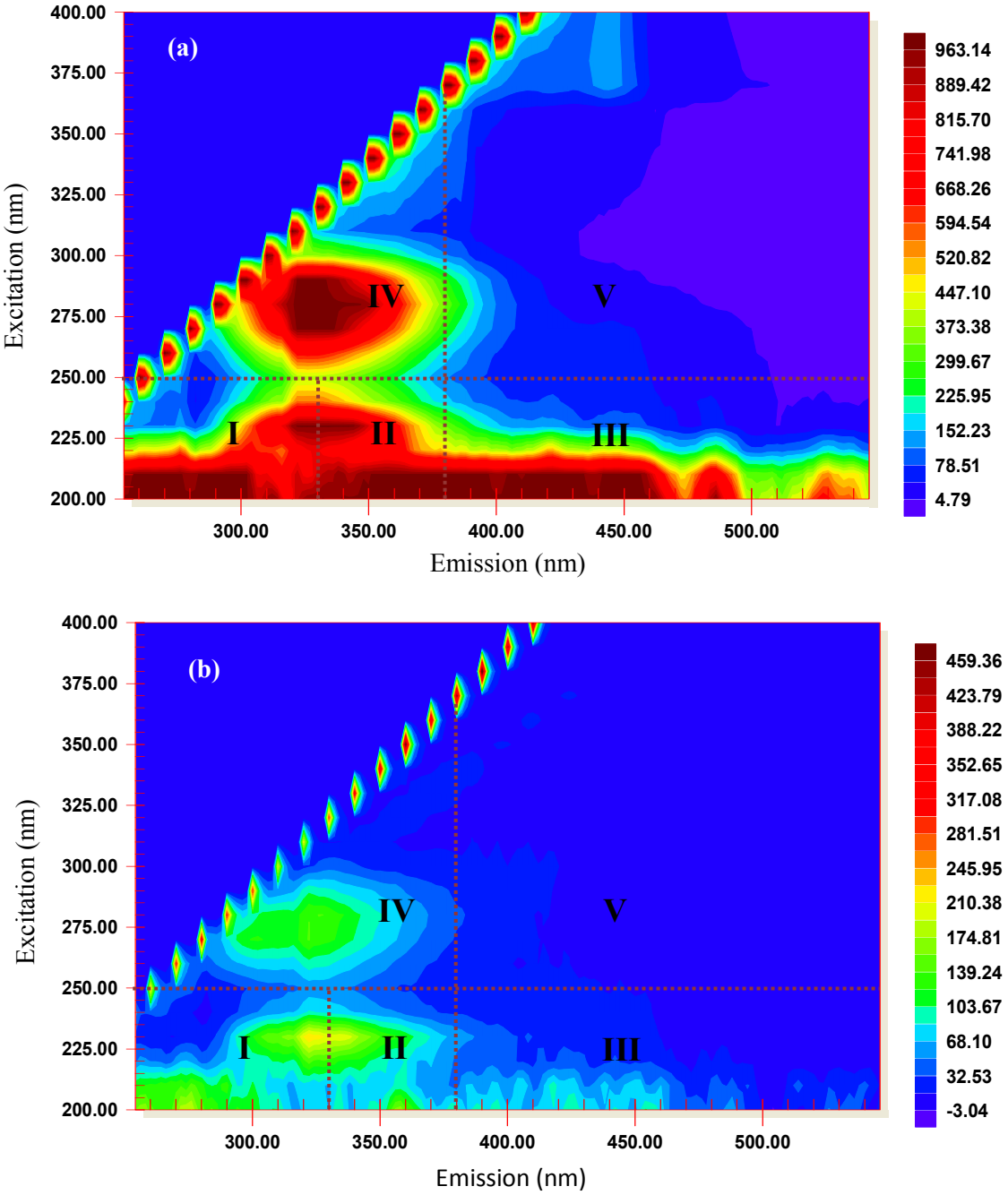

Figure 4.16 Fluorescent EEM of membrane fouling on HPI membrane operated under 60% critical flux in MBR-1. (a) In cake layer; (b) Inside of membrane pore

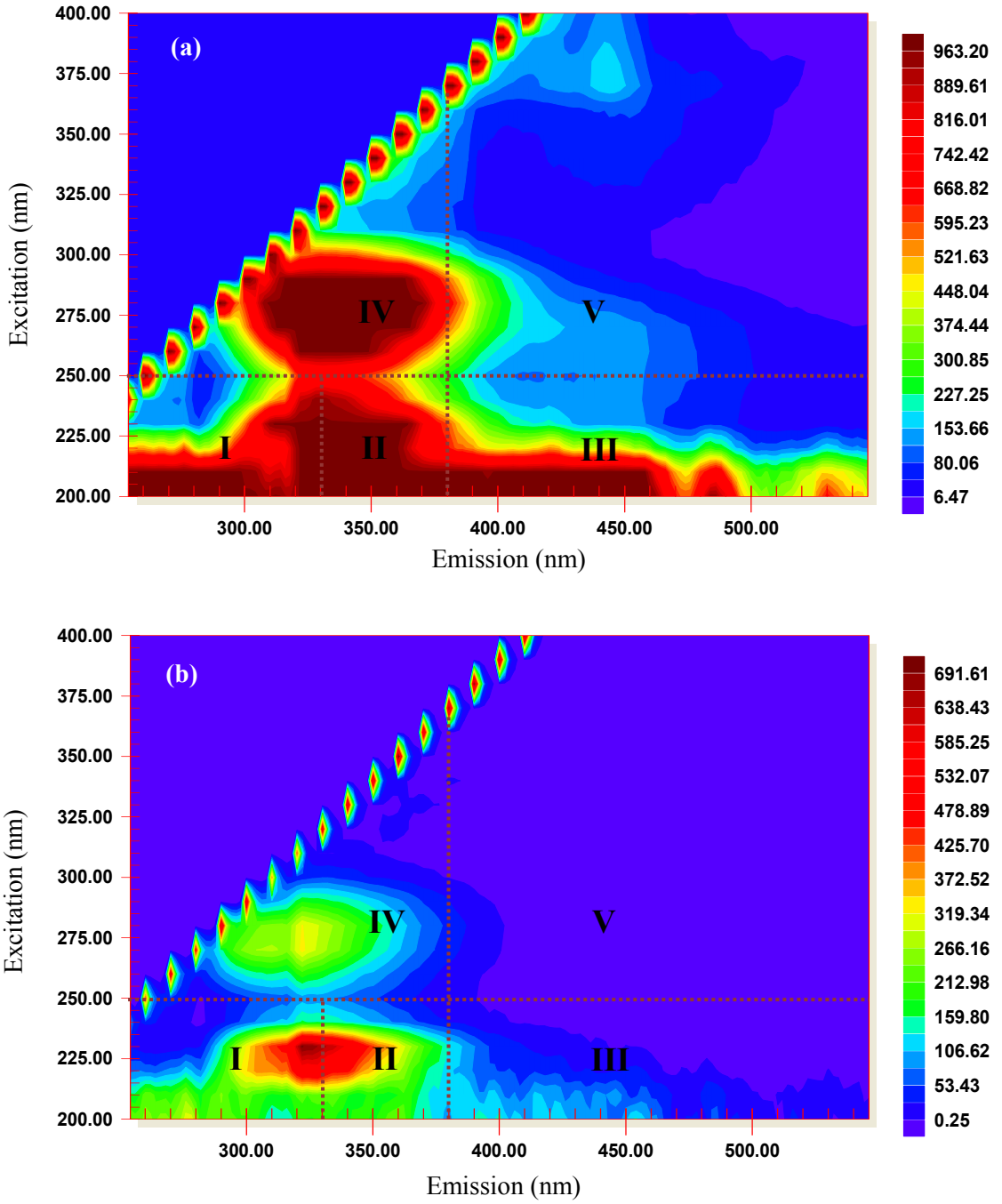

Figure 4.17 Fluorescent EEM of membrane fouling on HPI membrane operated under 80% critical flux in MBR-2. (a) In cake layer; (b) Inside of membrane pore

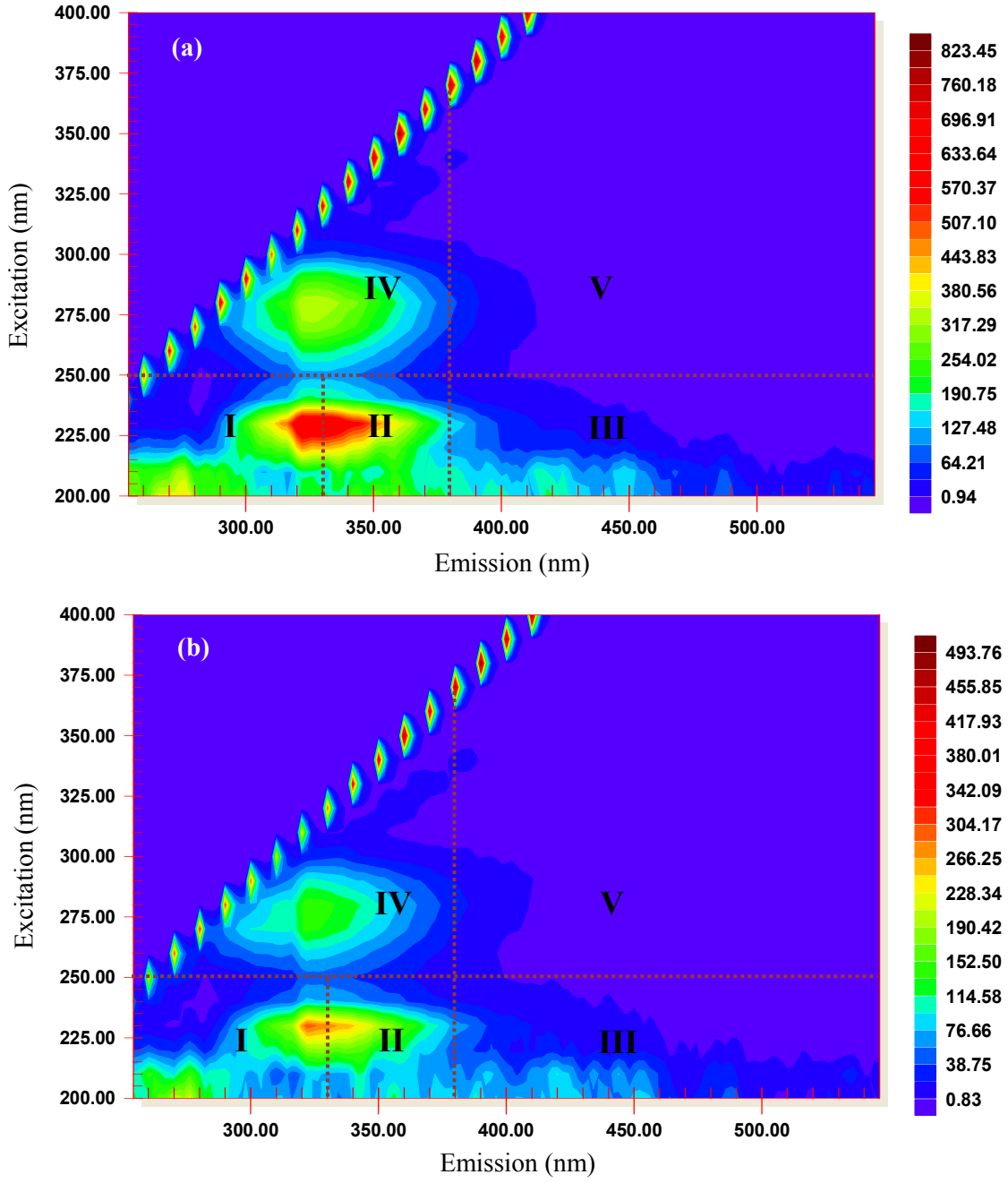

Figure 4.18 Fluorescent EEM of membrane fouling on HPO membrane operated under 80% critical flux in MBR-2. (a) In cake layer; (b) Inside of membrane pore

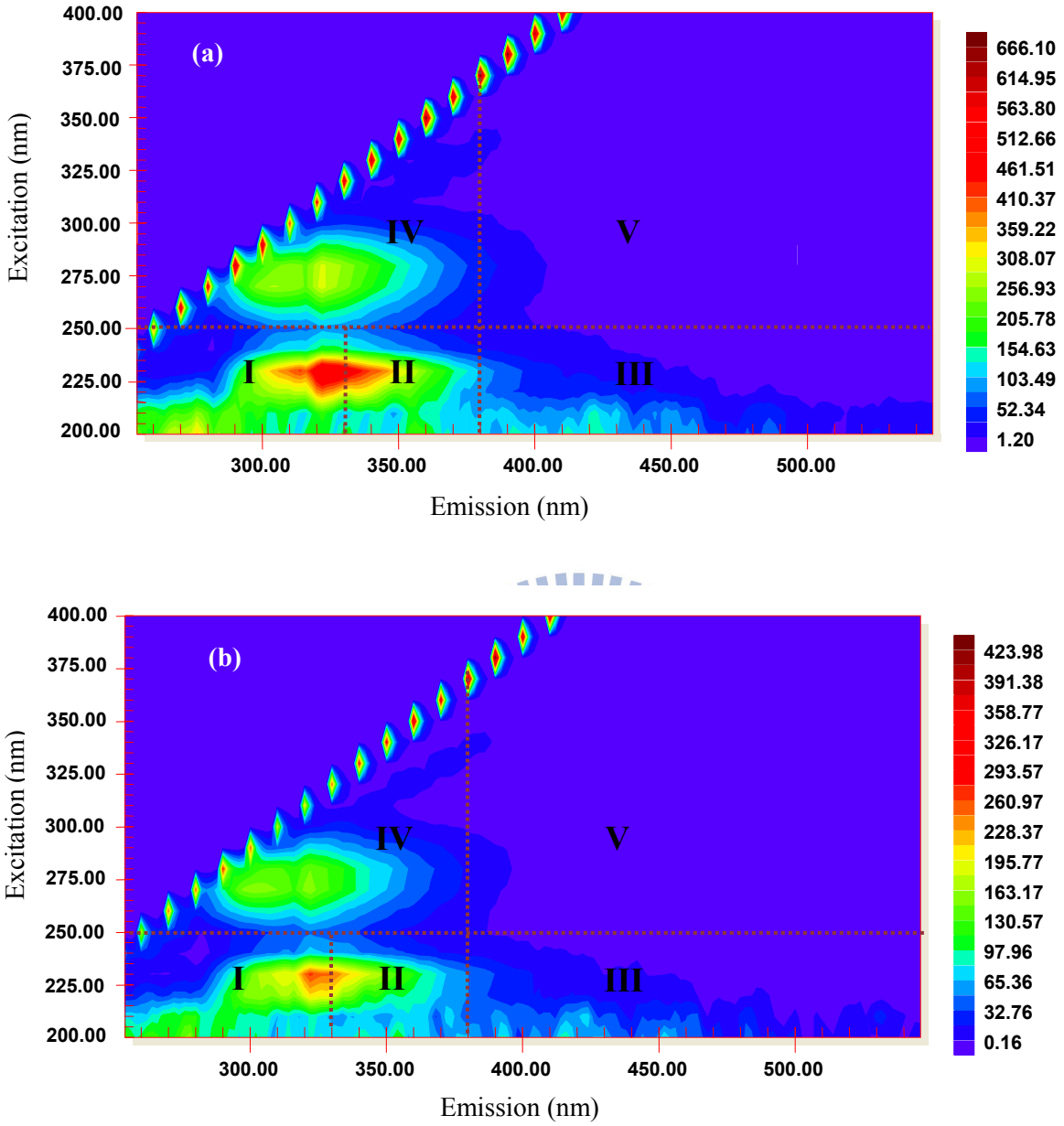

Figure 4.19 Fluorescent EEM of membrane fouling on HPI membrane operated under 60% critical flux in MBR-2. (a) In cake layer; (b) Inside of membrane pore

4.4.2 Characterization of fouling composition

Membrane fouling plays an important core role in MBR system effecting to wastewater treating efficiency. As introduced in Section 2.1.3, membrane fouling includes three basic types: adsorption, pore blocking and cake layer (Hong *et al.,* 2005). In which, cake layer contributes 80% of resistance (Lee *et al.,* 2001). Yet, cake layer compositions were concerned to compare the fouling behavior of four sub-critical fluxes operation. Besides, the fouling in the inner membrane pores was also studied. The extent of this section was to characterize the main fouling compositions represented as EPS and SMP. In which, EPS includes soluble EPS and bound EPS. SMP was considered as soluble EPS constituted by soluble polysaccharides and soluble proteins. Cell-bound polysaccharides and cell-bound proteins were identified as the compositions of bound EPS.

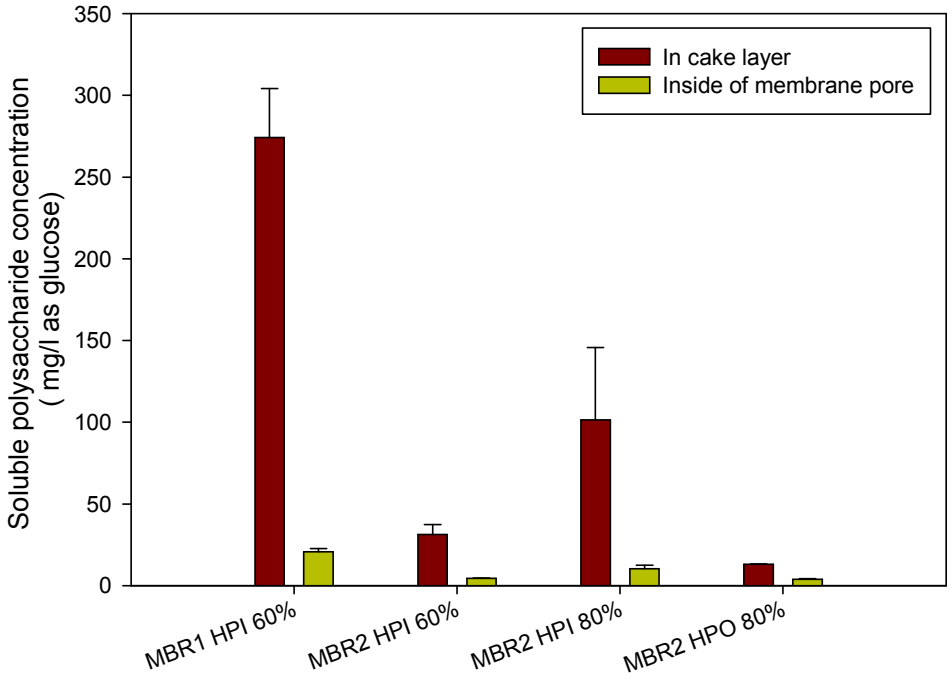

Figure 4.20 Soluble polysaccharides in cake layer and in membrane pore

Figure 4.20 shows the soluble polysaccharides in cake layer and inside of membrane pore of four operational cases in this study. That were HPI and HPO membranes operated under 80% of critical fluxes in MBR-2; and HPI membranes operated under 60% of critical flux in MBR-1 and MBR-2 (specific data were showed in Appendix 1). Soluble polysaccharides in cake layer and inside of membrane pore of HPI membrane operated under 60% of critical flux in MBR-1 were 274.1 and 20.74 mg/l as

glucose. It was relatively higher than that in MBR-2 with 31.34 and 4.36 mg/l as glucose. It indicates that the higher the activated sludge of MBR operated, the higher the soluble polysaccharides were.

In case of HPI membranes operated in MBR-2 with the different imposed sub-critical fluxes (60% and 80% critical flux), soluble polysaccharides in cake layer and inside membrane pore of 60% of critical flux operation (31.34 and 4.36 mg/l as protein, respectively) were lower than that under 80% critical flux operation (101.34 and 10.39 mg/l as protein, respectively). As a result, the greater soluble polysaccharides in cake layer and inside of membrane pore were presented at the higher imposed sub-critical flux operation. For the HPI and HPO membrane operated in the same conditions (in MBR-2 and under 80% of critical flux), soluble polysaccharides (in cake layer and inside of membrane) of HPO membrane (12.96 and 3.98 mg/l as glucose) was less than that in HPI membrane (101.34 and 10.39 mg/l as protein, respectively)

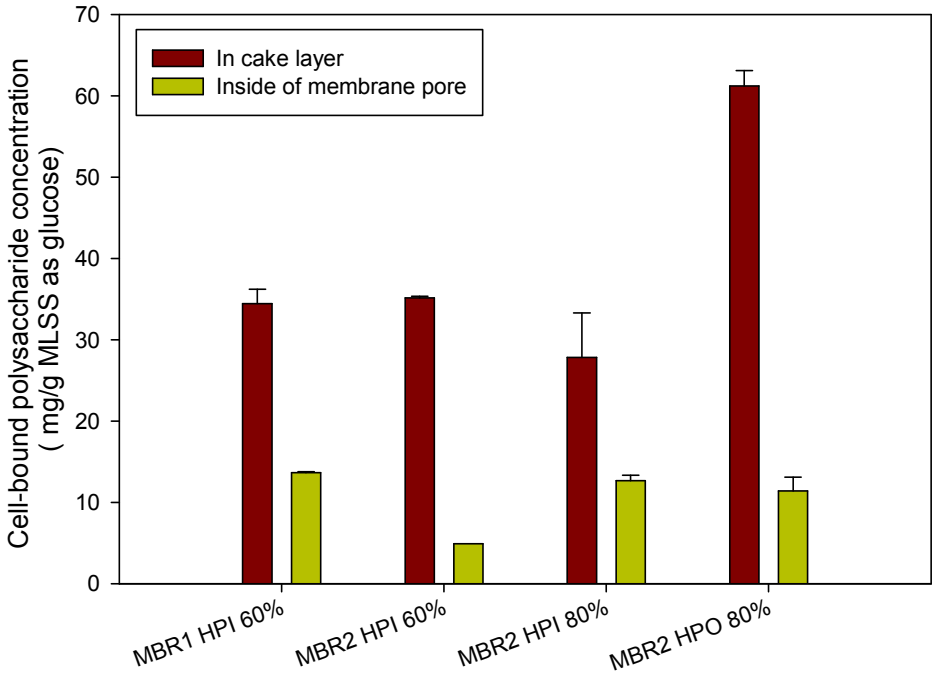

Figure 4.21 Cell-bound polysaccharides in cake layer and in membrane pore

Cell-bound polysaccharides in cake layer and inside of membrane pore were illustrated in Figure 4.21. Cell-bound polysaccharides in cake layer of HPI membranes (operated under 60% of critical flux) in MBR-1 were similar to in MBR-2 (approximately 35 mg/g MLSS as glucose). While for inside of membrane pore, it (13.66 g/ g-MLSS as

glucose) was higher than in MBR-2 (4.89 g/g-MLSS as glucose). In other case, cell-bound polysaccharides in cake layer of HPI membrane operated under the lower imposed sub-critical flux (60% of critical flux in MBR-2) was greater than that in 80% of critical flux while it was less than in the inner membrane. Regarding to the membrane fouling on HPI and HPO membrane operated under the similar conditions (operated under 80% of critical flux and in MBR-2), cell-bound polysaccharides seem to be the same in the inner membrane but in cake layer, it was pretty high for HPO membrane compared with HPI membrane.

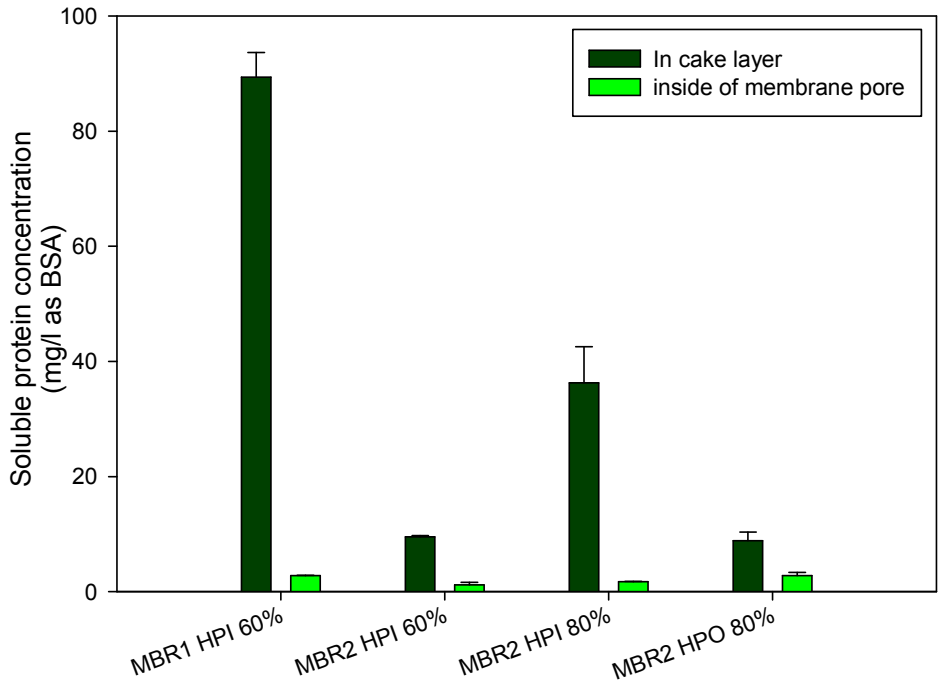

Figure 4.22 Soluble proteins in cake layer and in membrane pore

As shown in Figure 4.22~23, the soluble protein and cell-bound protein in cake layer and inside of membrane pore were clearly illustrated for each operational case to figure a correlation about protein as membrane fouling compositions between HPI and HPO membranes operated under 80% of critical flux in MBR-2 or HPI membrane operated under similar sub-critical flux (60% critical flux) but in different activated sludge concentration (in MBR-1 and MBR-2) or HPI membrane operated in the same activated sludge concentration (in MBR-2) but under different sub-critical fluxes (60% and 80% of critical fluxes) (specific data were shown in Appendix 2).

In particular, the soluble proteins in cake layer of HPI membrane operated under 60% of critical flux in MBR-1 (89.35 mg/l as Bovine Serum Albumin (BSA)) were pretty higher than that in MBR-2 (2.75 mg/l as BSA). In contrary, the cell-bound proteins in MBR-1 (25.59 mg/g MLSS as BSA) were lower than in MBR-2 (106.72 mg/g MLSS as BSA). In case of inside membrane pore, the soluble proteins of membrane in MBR-1were higher than in MBR-2 .But it was contrary with cell-bound proteins.

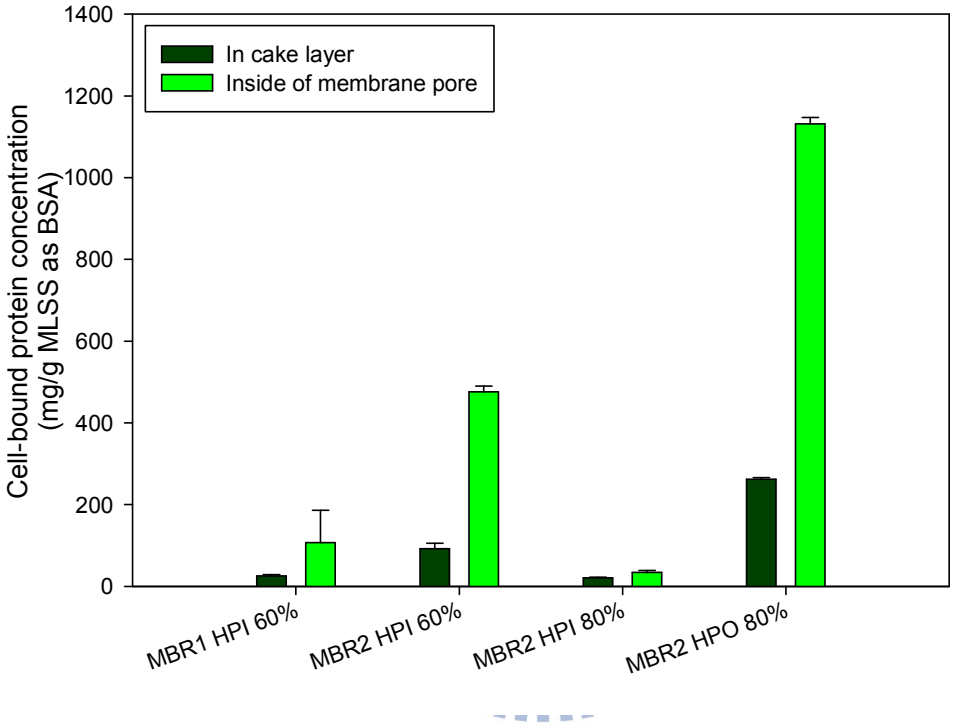

Figure 4.23 Cell-bound proteins in cake layer and in membrane pore

With the operation of HPI membranes in MBR-2 under different fluxes (60% and 80% of critical flux), soluble proteins in cake layer operated under sub-critical flux of 60% critical flux (9.56 mg/l as BSA) were less than that operated under 80% critical flux (1.16 mg/l as BSA). While for inside of membrane, it was higher. For the operation of HPI and HPO membranes with the same conditions (in MBR-2 and 80% critical flux), soluble proteins in cake layer were lower for HPI membrane and pretty higher for HPO membrane but inside of membrane pore.

A summary of membrane fouling compositions in different operational conditions was given in Table 4.5

Table 4.5 Summary of membrane fouling compositions in different operation conditions

	Operational conditions	60% critical flux HPI membrane		MLSS: 6,000 – 6,500 mg/l HPI membrane		MLSS: 6,000 – 6,500 mg/l 80% critical flux	
	Constituents	**MBR-1**	**MBR-2**	**60%**	**80%**	**HPI**	**HPO**
In cake layer	**Soluble polysaccharides**	Higher	Lower	Lower	Higher	Higher	Lower
	Cell-bound polysaccharides	Same	Same	Higher	Lower	Lower	Higher
	Soluble proteins	Higher	Lower	Lower	Higher	Higher	Lower
	Cell-bound proteins	Lower	Higher	Higher	Lower	Lower	Higher
Inside of membrane pore	**Soluble polysaccharides**	Higher	Lower	Lower	Higher	Higher	Lower
	Cell-bound polysaccharides	Higher	Lower	Lower	Higher	Same	Same
	Soluble proteins	Higher	Lower	Same	Same	Lower	Higher
	Cell-bound proteins	Lower	Higher	Higher	Lower	Lower	Higher

4.4.3 Distribution of fouling compositions in cake layer

From the CLSM images, protein, α-D-glucopyranose polysaccharides, of β-D-glucopyranose polysaccharides and DNA were represented by green color, cyan color, blue color and red color as shown in Figures 4.24~27. Figures 4.24~25 showed the presence of membrane fouling compositions on HPI and HPO membrane operated under 60% of critical flux in MBR-2. While for Figure 4.26~27, those compositions on HPI membranes operated under 80% of critical flux in MBR-2 and MBR-1 were given, respectively. In particular in Figure 4.24, images (a), (b), (c) and (d) show the presence of protein, α-D-glucopyranose polysaccharides, β-D-glucopyranose polysaccharides and DNA in membrane fouling on membrane surface, respectively. Image (e) shows the overlap image of membrane fouling. In general, it can be visibly seen that protein with green color are predominant compared to other substances for Figures 4.24~27. That means protein is the main constituent contributed to the fouling formation of membrane. Polysaccharides (α-polysaccharides and β-polysaccharides) also contribute to the formation of membrane even thought polysaccharides play a smaller role than protein.

By this CLSM tests, the thickness of cake layers were measured with 95.77 μm and 62.4 μm for HPI membranes operated in MBR-1 and MBR-2, respectively, under the same fluxes. For HPI and HPO membrane operated under 80% of critical flux in MBR-2, it was 101.51 and 76.93 μm, respectively.

The vertical distribution of membrane fouling compositions in cake layer was also observed. Figures 4.28~31 show the vertical distribution of protein, α-polysaccharides, β-polysaccharides and DNA. The changes of these substances were observed from the cake layer surface to the membrane surface corresponding from 0% to 100% of X axis. All substances were lower at membrane surface and higher at cake layer surface. However, the highest peaks lie between 40% and 80% of the depth of the cake layer. That means all the substances tend to be deposited at the middle of the cake layer. Especially, in case of membrane fouling on HPI membrane operated under 60% of critical flux in MBR-2, all the fouling compositions at cake layer surface are lower than that at membrane surface excepting the case of DNA

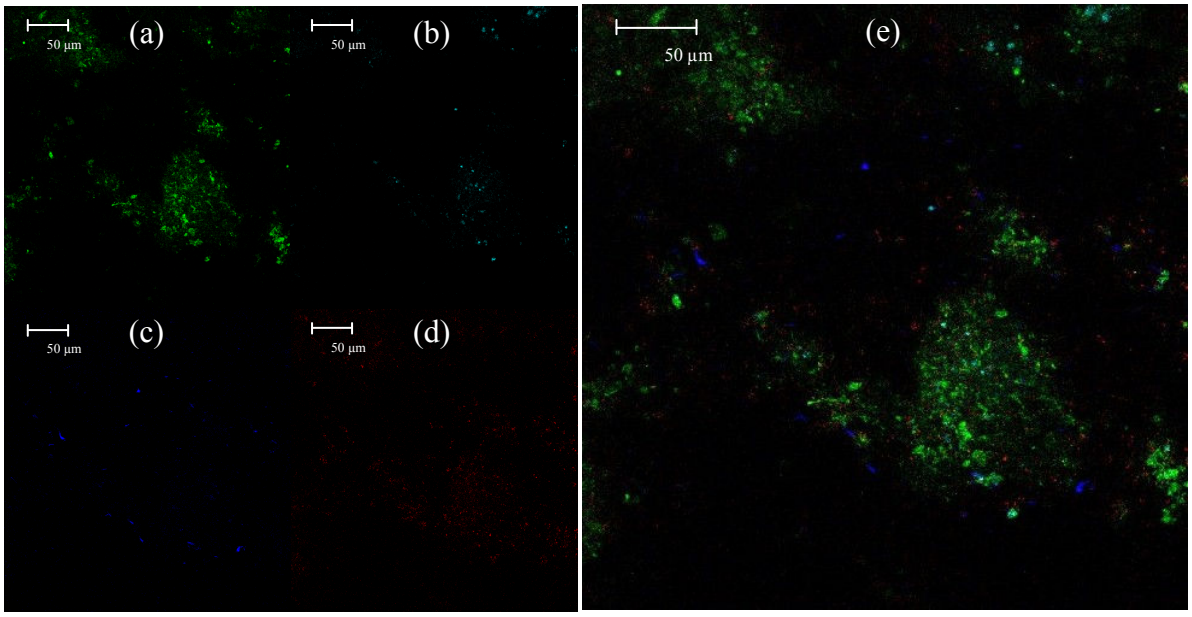

Figure 4.24 CLSM images of membrane fouling on HPI membrane operated under 60% critical flux in MBR-1 (a) CLSM image of protein (FITC); (b) CLSM image of α-D-glucopyranose polysaccharides (ConA); (c) CLSM image of β-D-glucopyranose polysaccharides (Calcoflour white); (d) CLSM image of DNA (SYTO 63); (e) CLSM overlap image

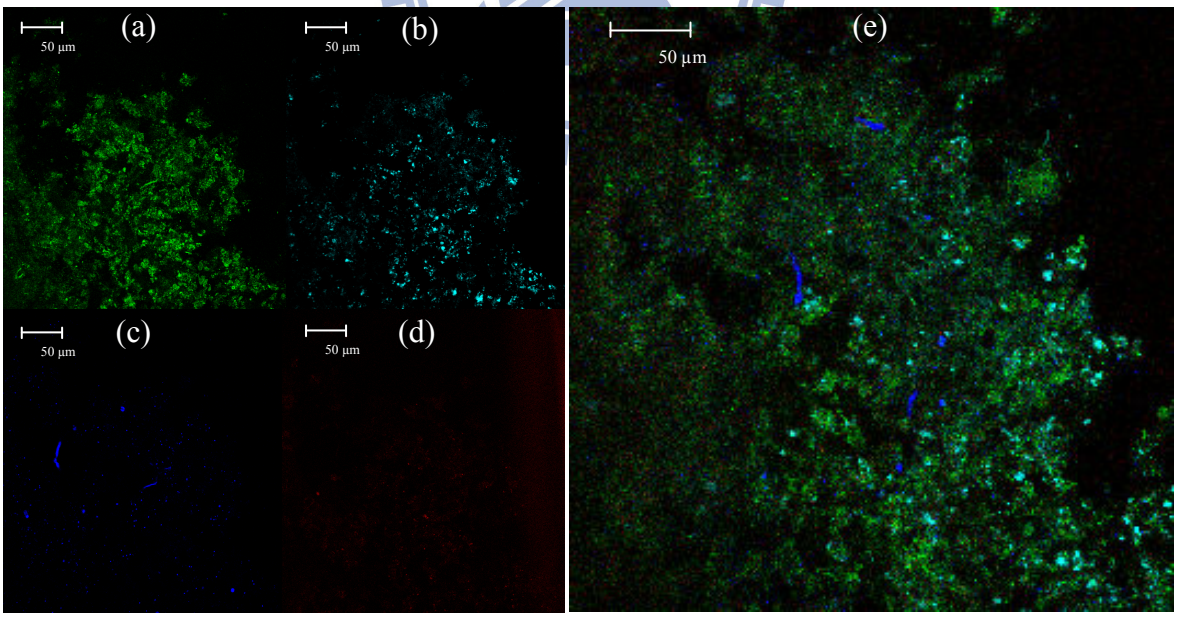

Figure 4.25 CLSM images of membrane fouling on HPO membrane operated under 80% critical flux in MBR-2 (a) CLSM image of protein (FITC); (b) CLSM image of α-D-glucopyranose polysaccharides (ConA); (c) CLSM image of β-D-glucopyranose polysaccharides (Calcoflour white); (d) CLSM image of DNA (SYTO 63); (e) CLSM overlap image

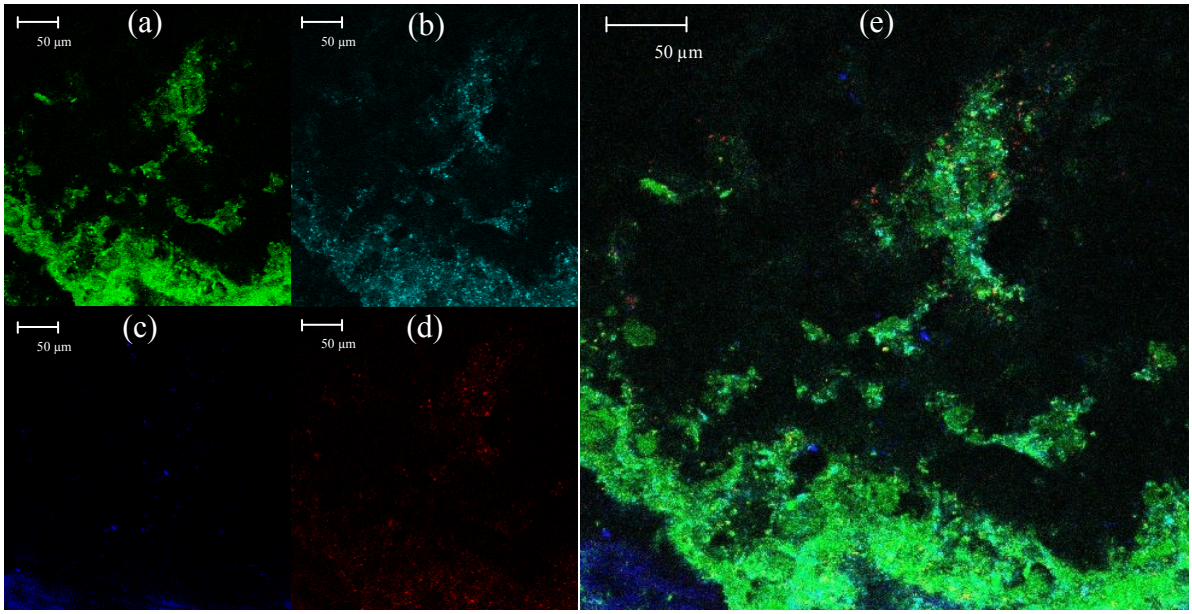

Figure 4.26 CLSM images of membrane fouling on HPI membrane operated under 80% critical flux in MBR-2 (a) CLSM image of protein (FITC); (b) CLSM image of α-D-glucopyranose polysaccharides (ConA); (c) CLSM image of β-D-glucopyranose polysaccharides (Calcoflour white); (d) CLSM image of DNA (SYTO 63); (e) CLSM overlap image

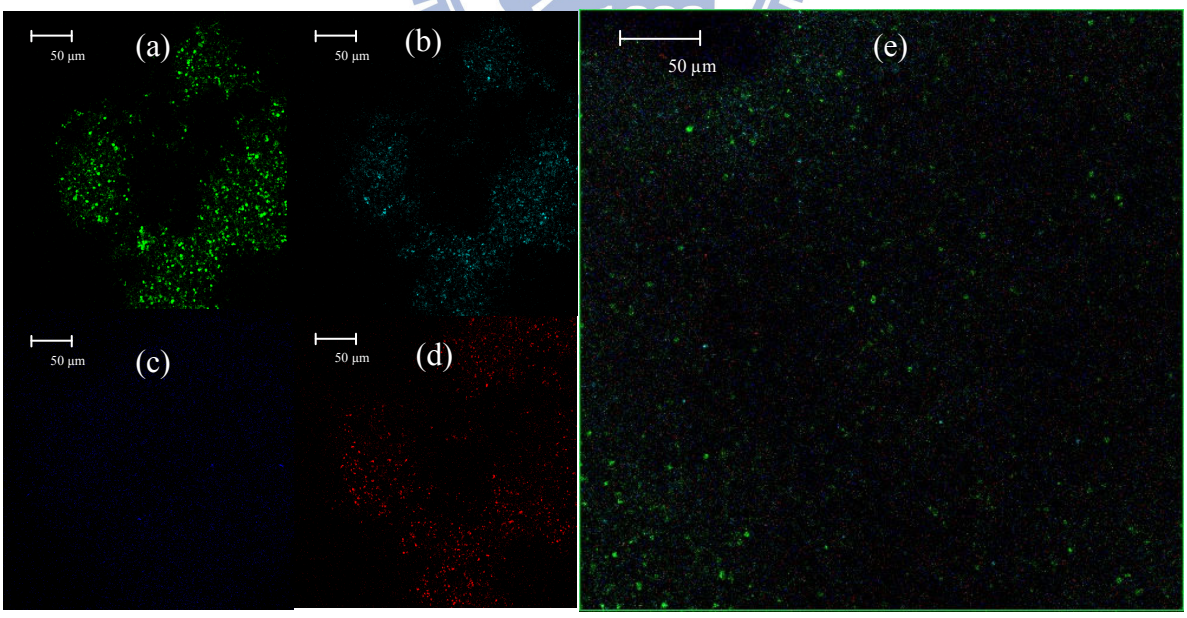

Figure 4.27 CLSM images of membrane fouling on HPI membrane operated under 60% critical flux in MBR-2 (a) CLSM image of protein (FITC); (b) CLSM image of α-D-glucopyranose polysaccharides (ConA); (c) CLSM image of β-D-glucopyranose polysaccharides (Calcoflour white); (d) CLSM image of DNA (SYTO 63) (e) CLSM overlap image

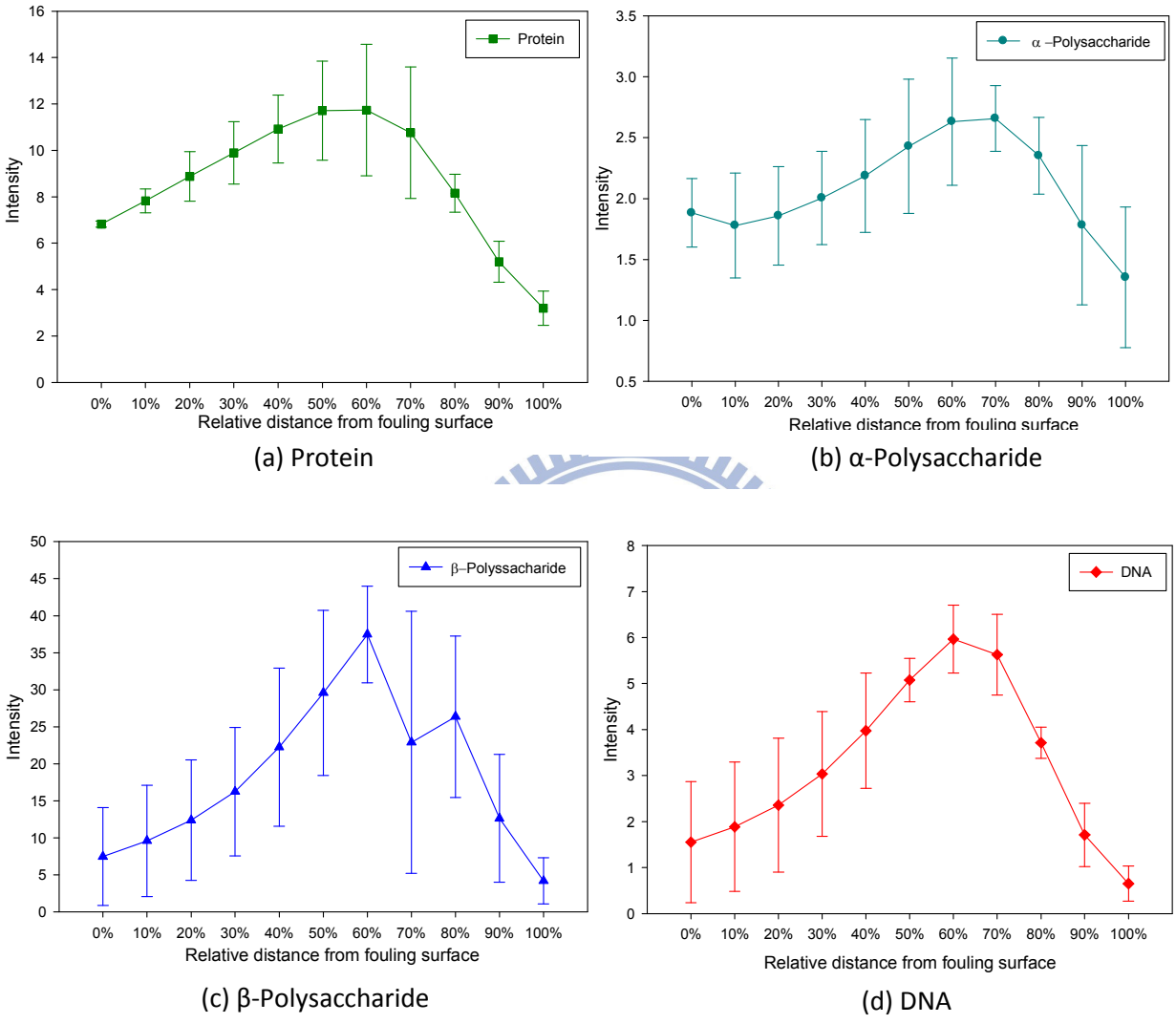

Figure 4.28 Vertical distribution of EPS in membrane fouling on HPI membrane operated under 60% critical flux in MBR-1

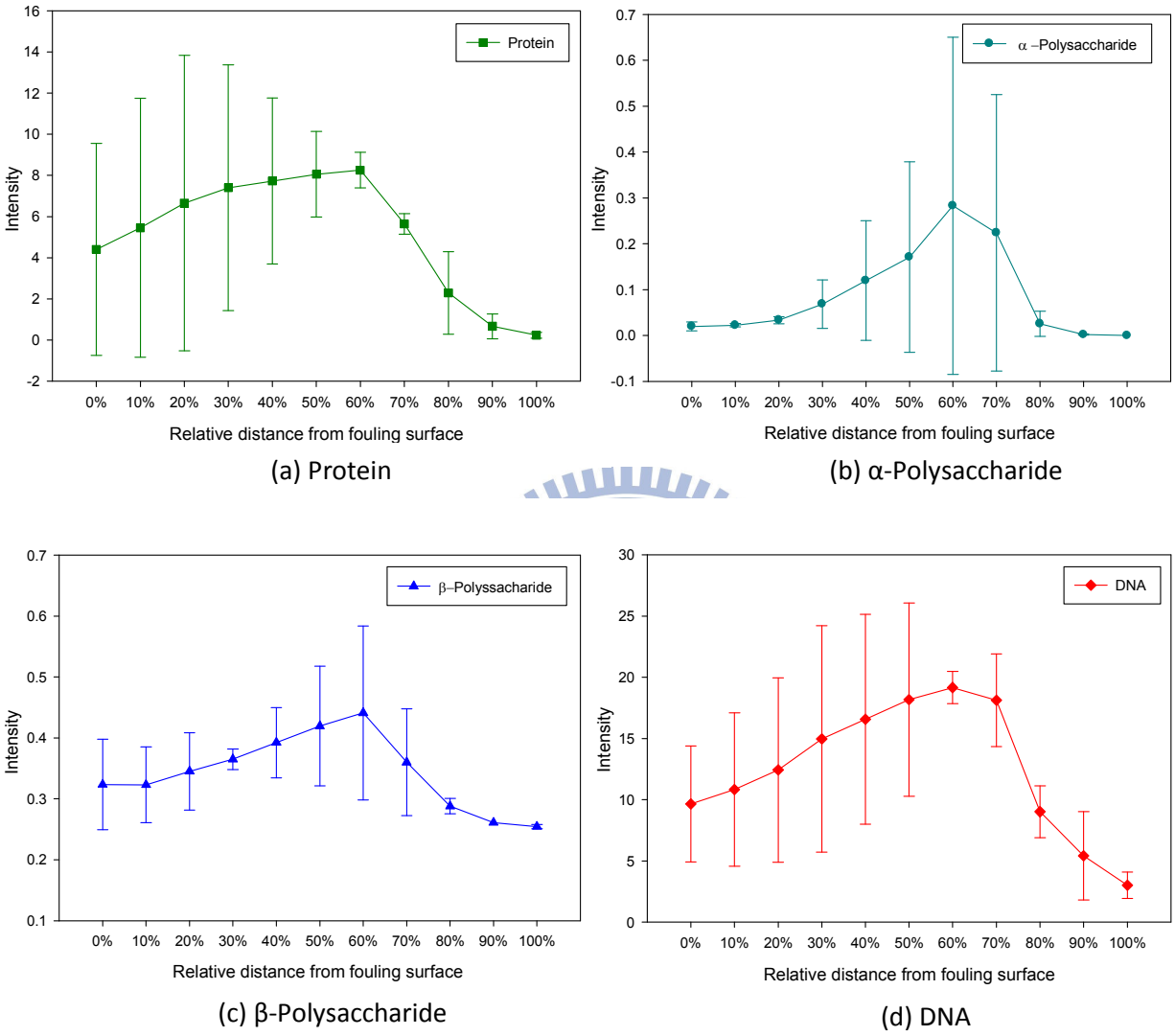

(a) Protein (b) α-Polysaccharide

(c) β-Polysaccharide (d) DNA

Figure 4.29 Vertical distribution of EPS in membrane fouling on HPO membrane operated under 80% critical flux in MBR-2

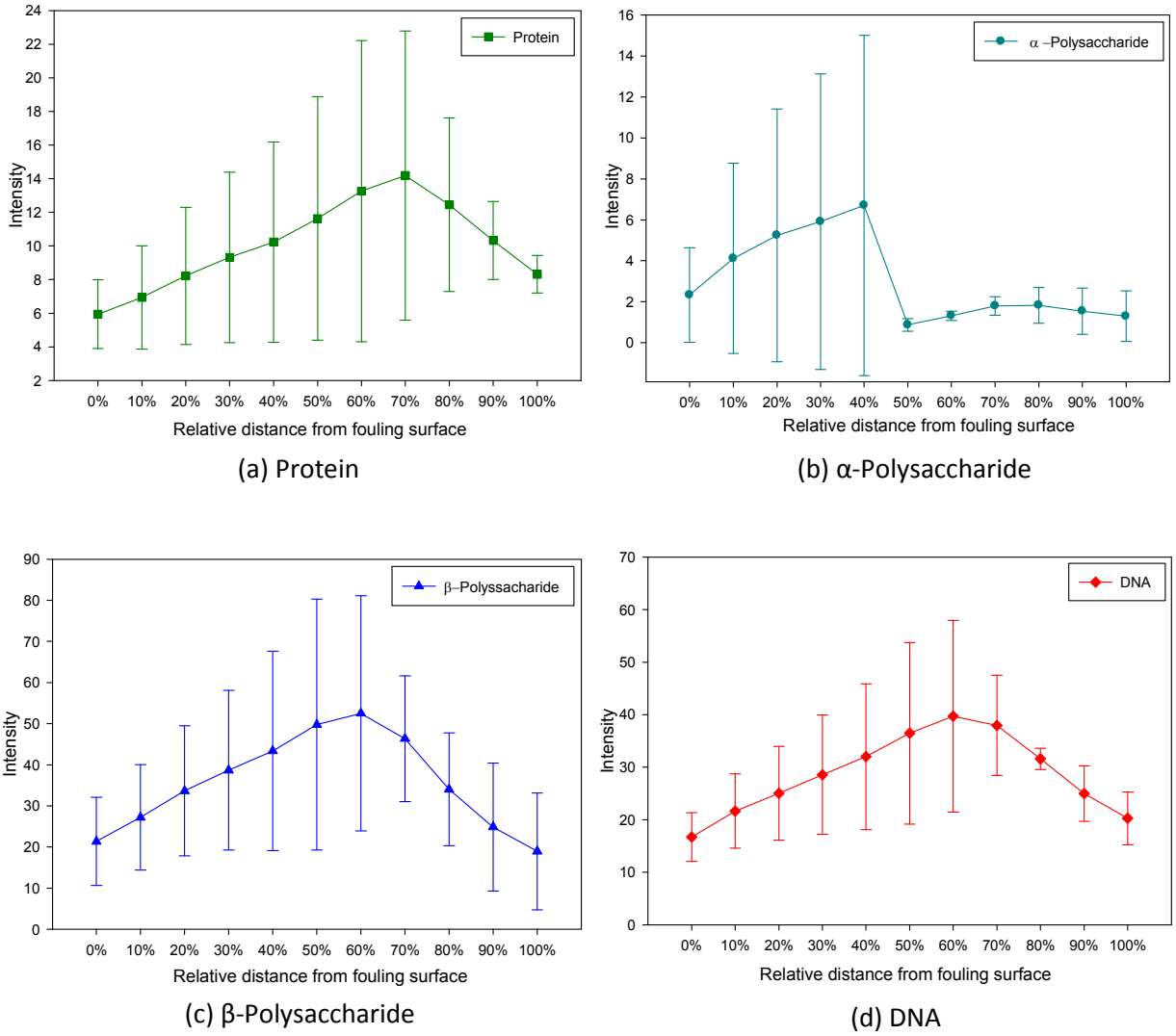

(a) Protein (b) α-Polysaccharide

(c) β-Polysaccharide (d) DNA

Figure 4.30 Vertical distribution of EPS in membrane fouling on HPI membrane operated under 80% critical flux in MBR-2

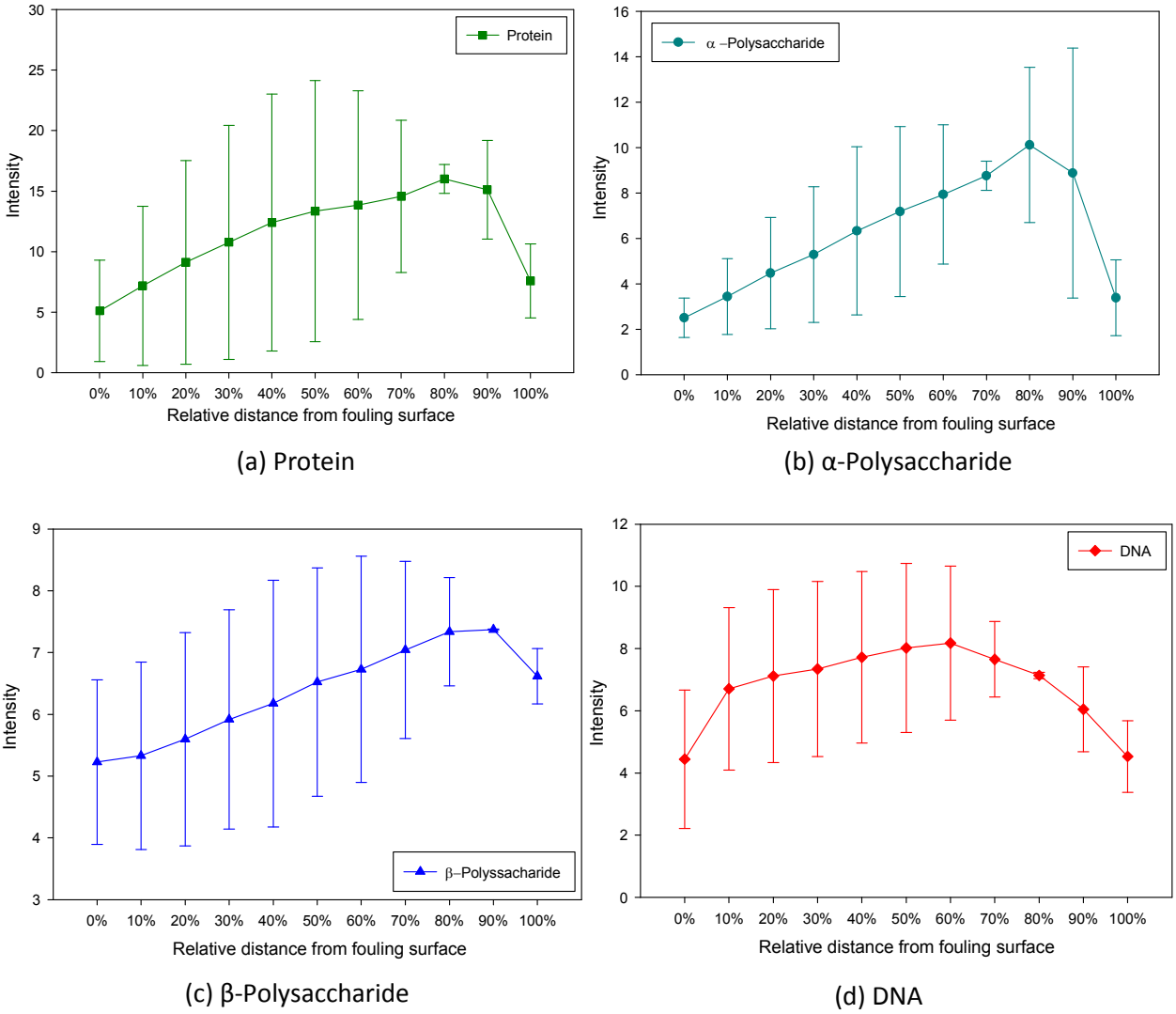

Figure 4.31 Vertical distribution of EPS in membrane fouling on HPI membrane operated under 60% critical flux in MBR-2

Chapter 5:

Conclusions and Recommendations

5.1 Conclusions

(1) Critical flux for HPI membrane operated with activated sludge of 7,000 – 7,500 mg/l, HPI and HPO membranes under 6,000 – 6,500 mg/l were found at 18, 33 and 30$lm^{-2}h^{-1}$, respectively.

(2) With the same membrane material, operation in a reactor with higher sludge concentration would cause a higher propensity of membrane fouling.

(3) HPO membrane could be easier fouled than HPI membrane in not only the short-term operation but also in the long-term operation.

(4) The higher the flux imposed, the faster the TMP jumped.

(5) The small particle size contributes to the fouling propensity.

(6) FTIR analysis shows the presence of proteins and polysaccharides in membrane foulants.

(7) EEM results show the presence of proteins in fouling as tyrosine-like aromatic protein and soluble microbial by-product-like protein. In which, operated in higher AS concentration caused the higher proteins concentration in both cake layer and membrane pore inside were. Otherwise, the higher flux imposed, the higher proteins in cake layer and membrane pore inside were also observed. Proteins in HPI membrane are higher than in HPO membrane.

(8) CLSM images show the presence of proteins, polysaccharides (α-polysaccharides and β-polysaccharides) and DNA. The thickness of cake layer were also measured with 95.77, 62.4 for HPI membranes operated under 60% of critical flux in MBR-1 and MBR-2. While for HPI and HPO membrane operated under 80% of critical flux in MBR-2, it was 101.51 and 76.93 μm, respectively.

(9) Vertical distribution analysis shows that the concentration of all substances on membrane surface is lower than on cake layer surface. They are mainly distributed at from 40% to 80% of the depth of cake layer.

5.2 Recommendations

(1) Further studies on membrane fouling under sub-critical flux operation is required.

(2) More investigation about the distribution of membrane fouling along the depth of cake layer should be concerned for understanding the fouling behavior.

(3) The effect of flux to the membrane fouling should be researched to analyze and solve economic problems in using MBR system.

References

Bradford, M.M. (1976) "A rapid and sensitive method for the quantitation of microgram quantities of protein utilizing the principle of protein-dye binding", *Analytical BioChemistry* **72**, 248-254.

Cardew, P.Y., and Le, M.S. (1998) Membrane Processes: A Technology Guide, The Royal Society of Chemistry

Chang, I.S., Le-Clech, P., Jefferson, B., and Judd, S. (2002) "Membrane fouling in MBRs for wastewater treatment", *Journal of Environmental Engineering* **128**(11), 1018-1029,

Chang, I.S., Lee, C. H., and Ahn, K. H. (1999) "Membrane filtration characteristics in membrane-coupled activated sludge system: The effect of floc structure on membrane fouling" *Separation Science and Technology* **34**, 1743-1758

Chen, W., Westerhoff, P., Leenheer, J.A., Brooksh, K. , (2003) "Fluorescence excitation-emission matrix regional integration to quantify spectra for dissolved organic matter", *Environmental Science and Technology* **37**, 5701-2710.

Chu, H.P., Li, X.Y. (2005) Membrane fouling in a Membrane bioreactor (MBR): Sludge cake formation and fouling characteristics, Wiley InterScience.

Dizge, N., Soydemir, G., Karagunduz, A., Keskinler, B. (2011) "Influence of type and pore size of membranes on cross flow microfiltration of biological suspension", *Journal of Membrane Science* **366**, 278-285.

Drews, A. (2010) "Membrane fouling in membrane bioreactors – Characterisation, contradictions, cause and cures", *Journal of Membrane Science* **363**, 1-28.

Dubois, M., Gilles, K.A., Hamilton, J.K., Rebers, P.A., and Smith, F. (1956) "Colorimetric method for determination of sugars and related substances" *Analytical Chemistry* 28, 350-356.

Espinasse, B., Bacchin, P., Aimar, P. (2002) "On an experimental method to measure critical flux in ultrafiltration", *Desalination* **146**, 91-96.

Field, R.W., Wu, D., Howell, J.A., and Gupta, B.B. (1995) "Critical flux concept for microfiltration fouling" *Journal of Membrane Science* **100**, 259-272.

Grube, M., Lin, J.G., Lee, P.H., Kokorevicha, S. (2006) "Evaluation of sewage sludge-based compost by FTIR spectroscopy", *Geoderma* **130**, 423-333.

Hong, S., Krishna, P., Hobbs, C., Kim, D., Cho, J. (2005) "Variations in backwash efficiency during colloidal filtration of hollow fiber microfiltration membranes", *Desalination* **173**, 257-268.

Howell, J.A. (1995) “Sub-critical flux operation of microfiltration”, *Journal of Membrane Science* **107**, 165-171.

Hwang, K.J., Liao, C.Y., Tung, K.L. (2008) “Effect of membrane pore size on the particle fouling in membrane filtration”, *Desalination* **234**, 16-23.

Jonsson, C., Jonsson, A.S. (1995) “Influence of the membrane material on the adsorptive fouling of ultrafiltration membranes”, *Journal of Membrane Science* **108**, 79-87.

Judd, S. (2006) The MBR book: Principles and Applications of Membrane Bioreactors in Water and Wastewater Treatment, Elsevier Ltd.

Kimura, K., Yamato, N., Yamamura, H., Watanabe, Y. (2005) “Membrane fouling in pilot-scale membrane bioreactors (MBRs) treating municipal wastewater”, *Environmental Science and Technology* **39**, 6293-9299.

Laspidou, C.S. and Rittman, B.E. (2002) “A unified theory for extracellular polymeric substances, soluble microbial products, and active and inert biomass” *Water Research* **36**, 2711-2720.

Le-Clech, P., Chen, V., and Fane, T.A.G. (2006) “Fouling in membrane bioreactors used in wastewater treatment”, *Journal of Membrane Science* **284**, 17-53.

Le-Clech, P., Jefferson, B., and Judd, S. J. (2003b) “Impact of aeration, solids concentration and membrane characteristics on the hydraulic performance of a membrane bioreactor”, *Journal of Membrane Science* **218**, 117-129.

Le-Clech, P., Jefferson, B., Chang, I.S., and Judd, S.J. (2003a) “Critical flux determination by the flux-step method in a submerged membrane bioreactor”, *Journal of Membrane Science* **227**, 81-93.

Liu, H., Fang, H.P. (2002) “Extraction of extracellular polymeric substances (EPS) of sludge”, *Journal of Biotechnology* **95**, 249-256.

Madaeni, S.S., Fane, A.G., Wiley, D.E. (1999) “Factors influencing critical flux in membrane filtration of activated sludge”, *Journal of chemical technology and biotechnology* **27**, 539-543.

Mafirad, S., Mehrnia, M.R., Azami, H. and Sarrafzadeh, M.H. (2011) “Effects of biofilm formation on membrane performance in submerged membrane bioreactors”, *Biofouling* **27**:5, 477-485.

Maximous, N., Nakhla, G., and Wan, W. (2009) “Comparative assessment of hydrophobic and hydrophilic membrane fouling in wastewater applications”, *Journal of Membrane Science* **339**, 93-99.

Meng, F., Chae, S.R., Drews, A., Kranume, M., and Shin, H. S. (2009) "Recent advances in membrane bioreactors (MBRs): Membrane fouling and membrane material", *Water Research* **43**, 1489-1512.

Pan, J.R., Su, Y.C., Huang, C.P. (2010) "Characteristics of soluble microbial products in membrane bioreactor and its effect on membrane fouling", *Desalination* **250**, 778-780.

Pollice, A., Brookes, A., Jefferson, B., Judd, S. (2005) "Sub-critical flux fouling in membrane bioreactors – a review of recent literate", *Desalination* **174**, 221-230.

Sheng, G.P., Yu, H.Q., Li, X.Y. (2010) "Extracellular polymeric substances (EPS) of microbial aggregates in biological wastewater treatment systems: A review", *Biotechnology Advances* **28**, 882-894.

Smith, C.W., Di Gregorio, D., and Talcott, R.M. (1969) "The use of ultrafiltration membranes for activated sludge separation", *Proceedings of 24th Annual Purdue Industrial Waste Conference*, Purdue University, West Lafayette, Indiana, USA, 1300-1310.

Stephenson, T., Judd, S., Jefferson, B., and Brindle, K. (2000) Membrane Bioreactors for Wastewater Treatment, IWA Publishing.

Tiranuntakul, M., Schneider, P.A., Jegatheesan, V. (2011) "Assessments of critical flux in a pilot-scale membrane bioreactor", *Bioresource Technology* **102**, 5370-5374.

Visvanathan, C., Ben Aim, R., and Parameshwaran, K. (2000) "Membrane separation bioreactors for wastewater treatment", *Critical Reviews in Environmental Science and Technology* **30:1**, 1-48.

Yamamoto, K., Hiasa, H., Talat, M., and Matsuo, T. (1989) "Direct solid liquid separation using hollow fiber membranes in activated sludge aeration tank", *Water Science and Technology* **21**, 43-54.

Zularisam, A.W., Ismail, A.F., Salim, R. (2006) "Behaviors of natural organic matter in membrane filtration for surface water treatment - a review." *Desalination* **194**, 211-231.

Appendix 1

Polysaccharide concentration in cake layer and in inside of membrane pore

			In cake layer		Inside of membrane pore	
Membrane	**Bioreactor**	**Percentage of critical flux (%)**	**Soluble (mg/l as glucose)**	**Bound (mg/g MLSS as glucose)**	**Soluble (mg/l as glucose)**	**Bound (mg/g MLSS as glucose)**
HPI	MBR-1	60	274.1 ± 30.03	34.43 ± 1.78	20.74 ± 1.78	13.66 ± 0.1
HPI	MBR-2	60	31.34 ± 5.88	35.14 ± 0.19	4.36 ± 0.15	4.89 ± 0.0
HPI	MBR-2	80	101.34 ± 44.31	27.83 ± 5.46	10.39 ± 2.1	12.67 ± 0.66
HPO	MBR-2	80	12.96 ± 0.26	61.21 ± 1.9	3.8 ± 0.33	11.42 ± 1.67

Appendix 2

Protein concentration in cake layer and in inside of membrane pore

			In cake layer		Inside of membrane pore	
Membrane	**Bioreactor**	**Percentage of critical flux (%)**	**Soluble (mg/l as BSA)**	**Bound (mg/g MLSS as BSA)**	**Soluble (mg/l as BSA)**	**Bound (mg/g MLSS as BSA)**
HPI	MBR-1	60	89.35 ± 4.31	25.59 ± 2.42	2.75 ± 0.07	106.72 ± 79.18
HPI	MBR-2	60	9.54 ± 0.19	92.14 ± 12.71	1.16 ± 0.46	475.81 ± 14.11
HPI	MBR-2	80	36.25 ± 6.29	21.09 ± 1.27	1.71 ± 0.04	34.4 ± 4.5
HPO	MBR-2	80	8.81 ± 1.51	262.26 ± 3.52	2.76 ± 0.56	1131.13 ± 16.38

Appendix 3

Polysaccharide and protein concentration in sludge and in the permeate of MBR-1 and MBR-2

		Glucose		Protein	
Bioreactor		**Soluble (mg/l as glucose)**	**Bound (mg/g MLSS as glucose)**	**Soluble (mg/l as BSA)**	**Bound (mg/g MLSS as BSA)**
MBR-1	Sludge	6.72 ± 0.48	32.58 ± 0.16	13.05 ± 0.35	26.12 ± 2.4
MBR-2	Sludge	5.39 ± 0.13	28.95 ± 3.39	4.2 ± 0.04	24.92 ± 0.57
MBR-1	Permeate	3.47 ± 2.78	-	1.66 ± 0.18	-
MBR-2	Permeate	3.3 ± 1.7	-	4.35 ± 0.78	-